Original Article
StAR-related lipid transfer domain protein 3 (STARD3) regulates HER2 and promotes HER2-positive breast cancer progression through interaction with HSP90 and SRC signaling

Doan Huu Nhat Binh[1,2], Tzu-Chun Cheng[3*], Shih-Hsin Tu[4*], You-Cheng Liao[5], Yi-Yuan Yang[6], Li-Ching Chen[7], Yuan-Soon Ho[3]

[1]Ph.D. Program in Medical Biotechnology, College of Medical Science and Technology, Taipei Medical University, Taipei, Taiwan; [2]Center of Prenatal - Neonatal Screening and Diagnosis, Hue University of Medicine and Pharmacy, Hue University, Thua Thien Hue, Vietnam; [3]Institute of Biochemistry and Molecular Biology, College of Life Science, China Medical University, Taichung 406040, Taiwan; [4]Department of Surgery, Taipei Medical University Hospital, Department of Surgery, School of Medicine, College of Medicine, Taipei Medical University, Taipei 110, Taiwan; [5]Graduate Institute of Medical Sciences, College of Medicine, Taipei Medical University, Taipei, Taiwan; [6]School of Medical Laboratory Science and Biotechnology, College of Medical Science and Technology, Taipei Medical University, Taipei 110301, Taiwan; [7]Department of Biological Science and Technology, College of Life Science, China Medical University, Taichung 406040, Taiwan. *Equal contributors.

Abstract: Although various HER2-targeted therapies have been approved clinically, drug resistance remains a considerable challenge. Studies have found that the cause of drug resistance is related to the expression of genes co-amplified with HER2 in breast cancer cells. Our study found that STARD3 was highly expressed in tumor tissues (n = 130, P < 0.001), especially in the HER2+ subtype (n = 35, P < 0.05), and correlated with poorer overall survival (HR = 1.47, P < 0.001). We discovered the interaction mechanism between STARD3 and HER2 proteins. We found that STARD3 overexpression increases HER2 levels by directly interacting with the HSP90 protein and inducing phosphorylated SRC, which may protect HER2 from degradation. Conversely, loss of STARD3 attenuates HER2 expression through lysosomal degradation. In addition, STARD3 overexpression induced cell cycle progression by inducing cyclin D1 and reducing p27. Therefore, the development of STARD3-specific targeted anti-cancer drugs would be helpful in the treatment of HER2+ patients. We further found that curcumin (15 μM) is a potent STARD3 inhibitor. STARD3-knockdown cells treated with curcumin (5 μM) showed a significant synergistic effect in inhibiting cancer cell growth and migration. The results suggest that targeting STARD3 would aid in treating HER2-positive breast cancer patients. This article uses curcumin as an example to prove that the targeted inhibition of STARD3 expression can be an option for the clinical treatment of HER2+ breast cancer patients.

Keywords: STARD3, MLN64, HER2, HER2-targeted therapy resistance, curcumin

Introduction

According to the GLOBOCAN report in 2022, breast cancer (BC) is the second leading cause of cancer-related mortality in United States women [1]. Despite attempts to develop new treatment strategies, a large proportion of breast cancer patients face recurrence and often metastasize. HER2-positive (HER2+) breast cancer is an aggressive subtype that comprises about 15-20% of all invasive breast carcinoma [2]. It is characterized by overex-pression of the tyrosine kinase receptor HER2 [2, 3]. Various HER2-targeted therapies, such as trastuzumab, pertuzumab, lapatinib, and neratinib, have shown promising results in treating HER2+ BC [4]. However, clinical cases have found that these drug treatments have failed cases. Suggests that other genes co-amplified with HER2 may be involved in signaling pathways and contribute to aggressive tumor progression [5, 6]. Therefore, finding reliable predictive markers of HER2+-mediated cancer development in combination with exist-

ing therapies would help reduce treatment failure [5, 7].

Recent studies identified more than 20 genes surrounding the smallest region amplicon of HER2 (17q12-21), several of which, including RARA, TOP2A, GRB7, and STARD3, were reported to be co-amplified with HER2 and may contribute to cancer progression [6, 8, 9]. Studies have shown that STARD3 is co-expressed with HER2 in many colorectal, gastric, and breast cancers [10-13]. However, it remains unclear how STARD3 enhances tumorigenesis and co-expresses and interacts with HER2 in breast cancer cells [14]. STARD3 is a StAR-related lipid transfer (START) domain-containing protein family member, localizes in late endosomes (LE), and has an essential function in the transportation of cholesterol between the endoplasmic reticulum (ER) to endosomes [15]. It was first found to be expressed in metastatic lymph node clone 64 (MLN64) in a screen for genes overexpressed in invasive breast cancer tissue [16]. Previous studies have shown that STARD3 is overexpressed in HER2+ BC cells [14, 17]. Conversely, knocking down STARD3 in HER2+ cancer cells reduces their growth [6, 17, 18], suggesting that STARD3 may be an important biomarker for HER2+ BC targeted therapy drug development [19, 20]. There are not many published data exploring the possibility of STARD3-targeted therapy. Two recent studies reported virtual studies of STARD3 inhibitors. Using ligand-based virtual screening, Chitrala et al. predicted ligands from the ZINC database with D(-)-Tartaric Acid inhibitor (PDB code: 1EM2) interrelates of the START domain of STARD3 [21]. Another inhibitor, VS1, was identified by Lapillo et al. using the "in silico" research platform [22]. Therefore, finding compounds that can inhibit STARD3 is a challenging task.

Natural compounds are potential therapeutic drugs due to their relative safety and synergistic effects in combination with clinical drugs to treat patients [23-25]. Several natural compounds, such as inotilone, EGCG, Curcumin, and phloretin, have received significant attention for their anti-cancer properties [25-27]. Curcumin, a polyphenolic compound found in turmeric, has been demonstrated to have several health benefits, such as antioxidant and anti-inflammatory capabilities [26, 28]. It has been reported to suppress the proliferation and growth of cancer cells by inhibiting many signaling pathways, including NF-κB activity, cyclin D, and PI3K/AKT [29, 30]. On the other hand, curcumin induces apoptosis by increasing the production of death receptors and caspases, activating the extrinsic apoptotic pathway [29, 31].

This study first confirmed that STARD3 is highly expressed in breast cancer tissues, especially in the HER2+ subtype. We also explored the relationship between STARD3 and HER2 at the protein level. We found that forcing STARD3 expression increased HER2 protein and promoted the growth of HER2+ cancer cells. Curcumin attenuates HER2 protein expression and synergizes with STARD3 knockdown to inhibit breast cancer cell proliferation. Through the study of the mechanism, we believe that in addition to HER2-targeted therapy for HER2+ breast cancer patients with high expression of STARD3, an appropriate dose of curcumin in the daily diet should help alleviate the disease.

Materials and methods

Chemicals and antibodies

Curcumin used in this study is a kind gift from Professor Min-Hsiung Pan, Institute of Food Sciences and Technology, National Taiwan University, Taipei, Taiwan.

The chemical used is Hygromycin B (catalog #J67371.XF, ThermoFisher Scientific, Waltham, Massachusetts, USA), G418 disulfate salt (catalog #4131, Bio-Techne, Minneapolis, MN, USA), Cycloheximide (CHX, 01810 Sigma-Aldrich, Germany), Bafilomycin A1 (BAF, 88899-55-2, Tocris, Bristol, UK).

The commercial antibodies shown below were purchased and used for western blotting, immunofluorescence (IF) staining, and IHC following the manufacturers' manual: anti-STARD3 (ab3478, Abcam, Cambridge, UK), anti-GAPDH (GTX627408, GeneTex, Irvine, CA, USA), anti-AKT (GTX121937, GeneTex, Irvine, CA, USA), anti-pAKT (#9271, Cell Signaling Technology, Beverly, MA, USA). The following antibodies were purchased from Santa Cruz Biotechnology, CA, USA: anti-HER2 (sc-33684), anti-HSP90 (sc-13119), anti-SRC (sc-8056), anti-pSRC (sc-166860), anti-Cyclin D1 (sc-83960), anti-p27 (sc-16410).

Cell culture

ATCC (American Type Culture Collection, Manassas, Virginia, USA) provided cell lines

such as BT474, HCC1954, SKBR3, AU565, T47D, ZR-75, MCF-7, BT483, MDA-MB-231, Hs-578T, HCC38, BT453, and MCF-10A, which were validated and certified. MCF-10A cells culture in DMEM/F12 with 20 ng/mL recombinant human EGF, 0.5 µg/mL hydrocortisone, 1x NEAA and 10 µg/mL insulin. All other cells were grown in DMEM/F12 containing 10% heat-inactivated FBS and 50 U/mL PSN. Cells were incubated in a 37°C incubator with 5% carbon dioxide CO_2.

Human patient samples

According to permission from the Taipei Medical University-Joint Institutional Review Boards, all patient samples (n = 153) were obtained at the Taipei Medical University Hospital, Taipei, Taiwan, as approved by the Institutional Review Board (IRB) and ethics committee of the institution (N202201070). The research was carried out under-recognized ethical standards. The clinical and pathological information on patient samples was obtained from the Taipei Medical University Joint Biobank.

Quantitative polymerase chain reaction (qPCR) analysis

Following the previous study [32], the procedure outlined was used for RNA extraction, reverse transcription, and qPCR. The Roche LightCycler LC2.0 was used for quantitative polymerase chain reaction following the manufacturer's instruction (Roche Molecular Biochemicals, Mannheim, Germany). The *STARD3* and *HER2* mRNA levels were examined using LightCycler v.4. Endogenous *GUS* mRNA expression was used to be normalized. The primers are listed in Table S1.

Construction of plasmids

STARD3 overexpression plasmid: Amplified the selected STARD3 sequence using PCR. The PCR conditions were 95°C for 5 min, 95°C for 50 s, 62°C for 10 s, and 72°C for 120 s in 35 cycles; finally, 72°C for 10 min. The STARD3-specific fragment was inserted into the pcDNA™5/TO vector (V103320, Thermo Fisher Scientific, USA) cut by *Hind*III and *Bam*H1 to generate the pcDNA™5/TO-STARD3 overexpression vector. The primers used are listed in Table S1.

STARD3 knockdown and scramble plasmid: Used BLOCK-iT™ RNAi Designer platform (at

https://rnaidesigner.thermofisher.com/rnaiexpress/) to predict the specific interference RNA to STARD3. The siRNA fragments are shown in Table S1.

These siRNA fragments were inserted into pSUPER.retro.neo-GFP plasmids (Oligoengine, Seattle, WA, USA) cut by *Bgl*II and *Hind*III restriction enzyme to generate the pSUPER-STARD3 siRNA vector and the pSUPER-STARD3 scramble vector.

Generation of stable cells

STARD3 stable overexpression cells: BT474 and SKBR3 cells were transfected with 1 µg of plasmid (empty plasmid for control and pcDNA™5/TO-STARD3 plasmid) using the Neon Transfection System (Thermo Fisher Scientific, USA). Hygromycin B (400 µg/ml) treated the transfected cells for 14 days. Then, the stable cells (BT474-OV, BT474-VT, SKBR3-OV, and SKBR3-VT) were established.

STARD3 knockdown stable cells: HCC1954 and BT474 cells were transfected with 1 µg of plasmid (pSUPER-STARD3 siRNA and the pSUPER-STARD3 scramble for control) using the Neon Transfection System (Thermo Fisher Scientific, USA). The transfected cells were treated with 500 µg/ml G418 disulfate salt. After 14 days of treatment, the stable cells (HCC1954-si, HCC1954-sc, BT474-si, BT474-sc) were established.

Wound healing assay

HCC1954 wild-type, scramble, and STARD3 knockdown stable cells were seeded with 10^4 cells in each well using Culture-Insert 2 Well. The fixed distance between the two wells is 0.5 mm. Images were captured at 0 and 12, 24, and 36 h using the Leica DMI 4000B System (Leica, Wetzlar, Germany). ImageJ software was used to measure the closure areas. The experiment was triplicated for the statistic.

Colony formation assay

Cells (HCC1954-WT, HCC1954-Sc, HCC1954-si, BT474-OV, BT474-VT, BT474-WT) were seeded at 300 cells in 3 cm culture dishes and incubated for 14 days. Cells were then fixed with 4% paraformaldehyde and stained with 0.5% crystal violet. The captured images were analyzed using ImageJ software. The experiment was triplicated for the statistic.

Immunofluorescence (IF) staining and Förster resonance energy transfer (FRET)

The experiment was performed following our previous report [32]. Cells (BT474-OV, BT474-WT, SKBR3-OV, SKBR3-WT, HCC1954-Sc, HCC1954-si, BT474-Sc, BT474-si) were stained with primary antibodies (anti-STARD3, anti-HER2, anti-HSP90). The secondary fluorescence antibody was used as an anti-rabbit-Rhodamine for anti-STARD3 and anti-mouse-FITC for anti-HER2 and anti-HSP90. Then, the slides were mounted using VECTASHIELD® Antifade Mounting Medium. The FRET method for photobleaching was performed following the manufacturer's instructions using the Leica TCS SP8 Confocal System (Leica, Wetzlar, Germany).

Flow cytometry analysis

SKBR3-OV and SKBR3-VT cells (n = 3) were cultured in a medium containing 0.04% FBS for 24 h to synchronize the cell cycle statuses. Cells were then replaced with a fresh medium containing 10% FBS and harvested at the time points (0, 3, 6, 9, 12, and 15 h). CytoFlex cytometer system (Beckman Coulter, USA) was used to collect flow cytometry data (10000 events), and CytExpert software (Beckman Coulter, USA) was used to analyze the proportion of each phase in the cell cycle.

Transwell migration assay

SKBR3-OV and SKBR3-VT cells were seeded at 10^4 cells into the upper chambers of the Transwell with the free FBS medium without Matrigel. 500 µL of DMEM/F12 medium supplement 10% FBS was added in the lower chambers and incubated for 24 h. The upper chamber was washed with FBS three times. Then, cells were fixed in 4% paraformaldehyde (Sigma Aldrich, USA) and stained with crystal violet 0.5%. The whole picture of the cells in the upper chamber bottom was captured using Leica DM500 Microscope with Microvisioneer ManualWSI scanner system. The experiment was triplicated for the statistic.

Immunohistochemistry (IHC) stain

The FFPE tumor sections from patients were heated at 60°C for 20 min and then deparaffinized in xylene for 15 min. After rehydrating with ethanol (100%, 90%, and 70% twice every 30 s, respectively), antigens were retrieved by boiling tumor sections in Tris EDTA (pH 9.0) buffer for 20 min. The sections were incubated with hydrogen peroxide 3% in methanol for 15 min and then blocked with BSA blocking buffer. Afterward, the primary antibodies (1:100) were used to incubate the sections for 4 h and secondary antibodies for 1 h. Then, immunostaining was applied using DAB-Substrate Chromogen System (K3468, Dako, Carpinteria, CA, USA), resulting in brown color in the antigen sites. After being stained with hematoxylin and dehydrated, the slides were mounted and sealed with a non-aqueous mounting medium.

Western blotting and immunoprecipitation assay

Cells were harvested on ice and extracted protein using golden lysis buffer (5 mM EDTA, 20 mM Tris-HCl pH 8.0, 10 mM NaF, 137 mM NaCl, 1% Triton X-100, 5 mM EGTA, and 10% glycerol), including protease inhibitors. Bradford assay (Bio-Rad) was used to examine the protein concentration. The same amount of protein lysates (35 µg) was loaded into 10% SDS-PAGE gel and electrophoresis. Protein was then transferred into a PVDF membrane (polyvinylidene fluoride, Millipore, Billerica, MA, USA) and blocked using 5% fat-free milk for 1 h. Membranes were incubated with the primary antibody at room temperature for 2 h and subsequently incubated with the HRP-conjugated secondary antibody at room temperature for 1 h, followed by ECL substrate (GE Healthcare), and finally captured by UVP BioSpectrum 500 Imaging System (Thermo Fisher Scientific, USA). The co-immunoprecipitation experiments involved using 1 mg of total protein extract from each cell sample. The protein extracts were incubated overnight with 2 µg of Hsp90 or HER2 antibody and then precipitated with protein A/G (Catalog #Topg-2, Biotools, Taipei, Taiwan). The cell extracts and the co-immunoprecipitated proteins were equally loaded and separated by SDS-PAGE, following the previously described protocol [33].

Calculate the coefficient of drug interaction

The coefficient of drug interaction (CDI) was used to examine the drug combination effect [34]. The formula is CDI = AB/(A × B), where AB is the ratio of the combined group to the control group. A, B is the ratio of the individual drug to

the control group. In our study, the knockdown of STARD3 was used as drug A effect, curcumin as drug B effect, and the combined curcumin treatment on STARD3 knockdown cells as AB. Regarding the combined use, CDI is compared to 1, where CDI < 1 indicates the synergism, = 1 is additive, and > 1 is antagonism. Especially CDI < 0.7 means the drugs have a strong synergism.

Cancer dataset TCGA, TNMplot, and Kaplan-Meier plotter analysis

Timer 2.0 of the TCGA database analyzed STARD3 expression in breast cancer and other cancers (http://timer.cistrome.org/) [35]. TNMplot analysis of STARD3 expression between normal, tumor, and metastatic gene array data, RNA-seq from TCGA, and microarray from GEO (https://tnmplot.com/analysis/) [36]. The correlation between STARD3 and HER2 expression was also analyzed using this platform. Overall Survival (OS), Recurrence-Free Survival (RFS), and Distant Metastasis-Free Survival (DFMS) in breast cancer were analyzed using Kaplan-Meier Plotter (https://kmplot.com/, reference number 202991_at) [37]. The LinkedOmics platform (http://linkedomics.org/) was used to analyze the correlation between STARD3 with different genes in breast tumors [38]. STARD3 expression in cell lines was referenced using the Genevisible database platform (https://genevisible.com/search, reference number 202991_at).

Statistical analysis

All data showed as mean ± SD of three or more independent replicates. The comparisons in *STARD3* mRNA levels in pair tumor and normal tissues were calculated using the Chi-square statistic. The two-tailed Student t-test was used to compare the groups. The *p* values were calculated using One-way ANOVA. The GraphPad Prism 8.3 software and IBM SPSS v.20 were used for statistical comparisons to calculate the *p* values, and less than 0.05 indicated significant statistics.

Results

STARD3 was preferentially expressed in human HER2+ breast tumors and HER2+ breast cancer cell lines

Recent studies have shown that STARD3 belongs to the minimal amplicon and is frequently co-amplified with HER2 [5, 6]. Therefore, we hypothesized that STARD3 expression might be associated with HER2 in BC tumors. We performed quantitative real-time PCR to test this hypothesis to assess STARD3 mRNA expression levels in 153 pairs of BC tumors and nearby normal tissues. **Table 1** shows the association of STARD3 with BC molecular subtypes, clinical parameters, and demographic information. The PCR amplification curves in the tumor tissues were "left-shifted" (**Figure 1A**, red lines) compared to the profiles in the normal tissues (green lines), indicating that the tumor samples had more STARD3 mRNA overall. The data was then divided into two groups (N > T, n = 23/153, 15% vs. N < T, n = 130/153, 85%; N = normal, T = tumor) according to the STARD3 mRNA expression pattern. The results indicated that the expression of STARD3 was significantly higher in the N < T group compared to the N > T group (**Figure 1B**). Further analysis revealed that HER2+ tumors showed a higher expression of STARD3 than HER2- tumors (**Figure 1C**). Immunohistochemistry (IHC) was performed on breast cancer (BC) tissues to confirm the expression pattern of STARD3. **Figure 1D** revealed a significant increase in STARD3 immunostaining in HER2+ tumor tissues compared to triple-negative breast cancer (TNBC). Moreover, HER2+ cell lines exhibited elevated levels of STARD3 expression compared to luminal and TNBC cell lines, and MCF-10A was used as a normal cell (**Figure 1E**). These observations suggest a positive correlation between STARD3 expression and HER2 expression in BC cell lines and breast tumors.

High expression of STARD3 in tumors is closely associated with HER2 expression and poor prognostic outcome

We further explored the correlation between the high expression of STARD3 and the disease process and prognosis of BC patients with the database. The Timer 2.0 analyzer [35] was used to analyze STARD3 and HER2 mRNA expression in a multi-cohort study. We found that STARD3 mRNA was considerably higher in several cancers, including breast cancer, compared to normal tissues (**Figure 2A**). Remarkable, STARD3 levels were higher in HER2+ subtype BC tumors than in other subtypes (basal, luminal). TMNplot analysis [36] in the TCGA RNA-seq database indicated that STARD3 was highly expressed in both tumor and metastatic tissues (**Figure 2B**). Similar observations were

Table 1. Clinical parameters and fold differences in STARD3 mRNA expression in paired tumor/normal samples

Parameter	N > T Group		N < T Group		χ^2	p value
	n	Mean ± SE	n	Mean ± SE		
1. Age					0.259	0.611
< 55	13	1.75 ± 0.48	66	6.38 ± 0.74		
≥ 55	10	2.31 ± 0.51	64	8.61 ± 1.33		
2. ER					1.483	0.223
Negative	3	1.72 ± 0.46	32	6.74 ± 1.18		
Positive	20	2.03 ± 0.4	98	7.85 ± 0.94		
3. PR					0.049	0.824
Negative	8	2.04 ± 0.58	48	6.93 ± 0.86		
Positive	15	1.97 ± 0.45	81	7.86 ± 1.11		
4. HER2					5.535	0.019
Negative	22	1.84 ± 0.33	95	6.65 ± 0.69		
Positive	1	5.24	35	10.09 ± 2.08		
5. TNBC					0.043	0.836
TNBC	3	1.72 ± 0.46	15	5.33 ± 1.48		
Non TNBC	20	2.03 ± 0.4	115	7.87 ± 0.84		
6. Pathology					0.695	0.874
D.C.I.S	1	0.9	3	10.59 ± 3.82		
I.D.C	19	2.18 ± 0.41	114	7.65 ± 0.85		
M.C	1	1.5	3	8.72 ± 2.57		
I.L.C	1	1.05	5	6.08 ± 3.22		
7. N					3.732	0.155
N0	12	1.65 ± 0.49	46	7.11 ± 1.55		
N1	3	2.34 ± 1.45	37	6.73 ± 1.20		
N2	0		15	7.11 ± 1.99		
N3	1	2.61	11	11.25 ± 2.73		
8. Stage					5.09	0.165
Stage I	12	1.65 ± 0.49	46	7.11 ± 1.55		
Stage II	5	1.98 ± 0.85	40	7.40 ± 1.23		
Stage III	1	1.44	26	7.98 ± 1.42		
Stage IV	2	2.61 ± 0.002	16	9.34 ± 2.04		
9. Grade					0.859	0.651
Grade 1	2	4.23 ± .083	19	7.42 ± 1.53		
Grade 2	13	1.99 ± 0.52	63	7.68 ± 0.94		
Grade 3	7	1.52 ± 0.31	45	7.46 ± 1.64		

S1A, S1B), with a correlation coefficient of 0.8335 (Figure S1C).

Furthermore, HCC1954 and BT-474 are in the top 10 cell lines with the highest STARD3 expression in the Genevisible database analysis (Figure S1D). These results are consistent with data from western blot analysis of various cell lines (**Figure 1E**). Next, we analyzed the prognostic value of STARD3 mRNA expression using the Kaplan-Meier plotter database [39] to compare the clinical outcomes of all breast cancer patients by upper quartile. As shown in **Figure 2F**, high expression of STARD3 in BC tissues was associated with poorer overall survival (OS), recurrence-free survival (RFS), and distant metastasis-free survival (DMFS). These results confirmed that STARD3 and HER2 expression was significantly associated with poor prognostic outcomes in BC patients.

Overexpression of STARD3 promotes HER2 cell proliferation, cell migration, and colony formation

Recent studies demonstrated that STARD3 might contribute to the progression and metastasis of HER2+ cancer cells [19, 40]. To understand the mechanism of STARD3 overexpression-enhanced HER2+ cell proliferation and migration, BT474 and SKBR3 cells were selected as cell study models. We established stable STARD3 overexpressing cell lines (BT474-OV and SKBR3-OV). Empty vector-transfected cell lines were used as controls (BT474-VT and SKBR3-VT) (**Figure 3A**). Cell proliferation assays were performed using the trypan blue assay. As shown in **Figure 3B**, STARD3 overexpression in both BC cells significantly promoted cell growth compared with wild-type and empty vector cells. In addition, the clonogenicity of STARD3-OV cells was assessed. The results

obtained in the GeneChip data of the GEO database (**Figure 2C**). Pearson correlation coefficient and regression showed that STARD3 and HER2 mRNA expression were correlated in tumor (0.8, **Figure 2D**) and normal tissues (0.71, **Figure 2E**), respectively. We explored more TCGA datasets using the LinkedOmics platform to validate this observation [38]. Heatmap and volcano plot again confirmed that STARD3 had the highest correlation with HER2 expression in invasive breast cancer (Figure
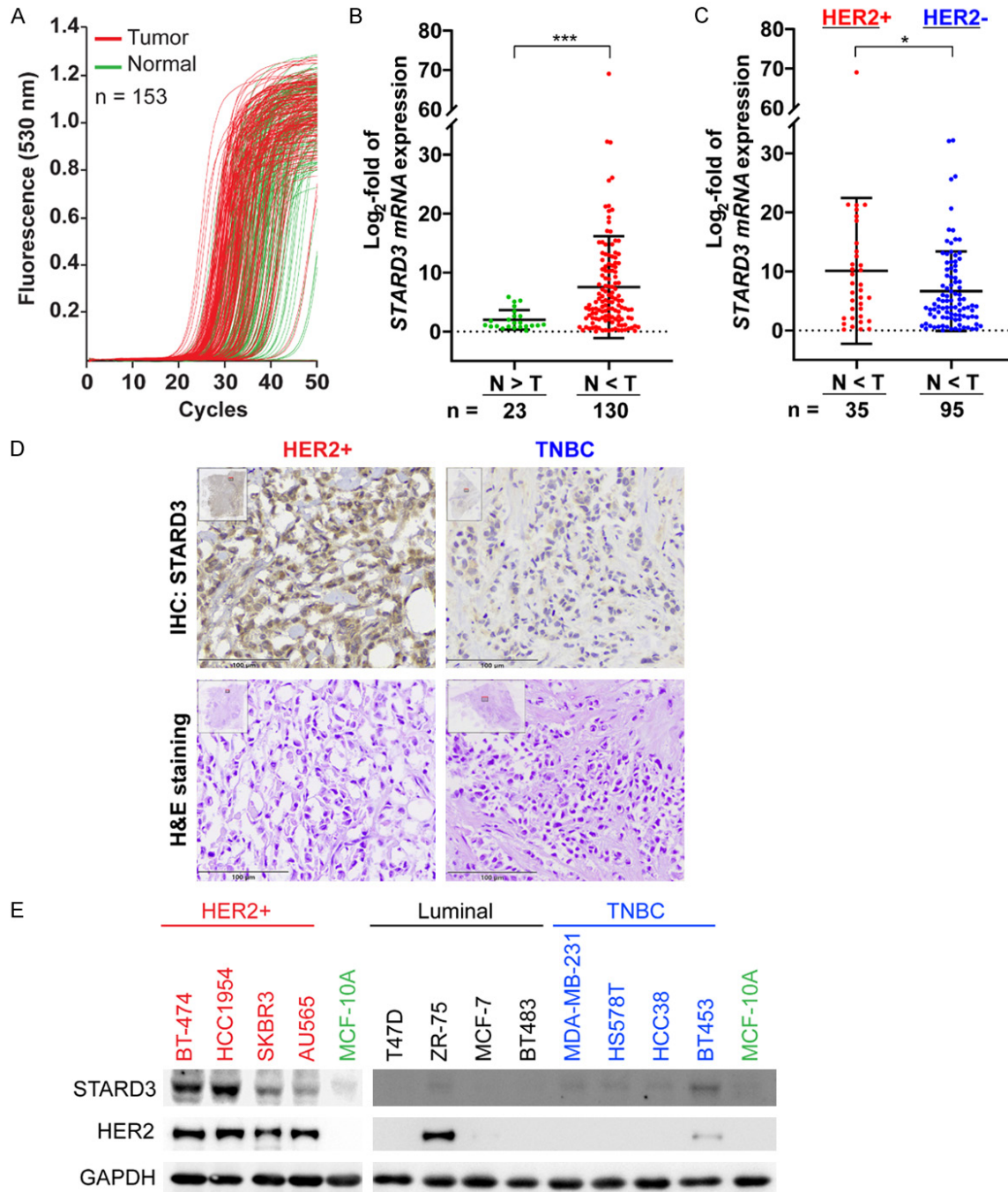
Figure 1. STARD3 overexpression in human HER2+ breast tumors and HER2+ BC cell lines. (A) Quantitative real-time PCR to evaluate STARD3 mRNA expression level in 153 pairs of tumors (red lines) and adjacent normal tissues (green lines) from BC patients. (B) Based on the STARD3 mRNA expression pattern, the qPCR data in (A) were separated into 2 groups: N > T group and N < T group (N = normal, T = tumor). (C) The N < T group data in (B) were subdivided into HER2+ and HER2- groups. (D) IHC staining observed STARD3 protein expression in HER2+ and TNBC tumor tissues. (E) Western blot results observed STARD3 protein expression in HER2+, luminal, or TNBC cell lines. The p values were calculated using the Student t-test ($*P < 0.05$, $***P < 0.001$).

indicated that STARD3 overexpression in BT474-OV cells significantly enhanced colony formation compared to controls (**Figure 3C**). STARD3 overexpression in SKBR3-OV cells sig- nificantly increased the number of migrated cells by Transwell migration assay compared to wild-type and vector groups assessed (**Figure 3D**).
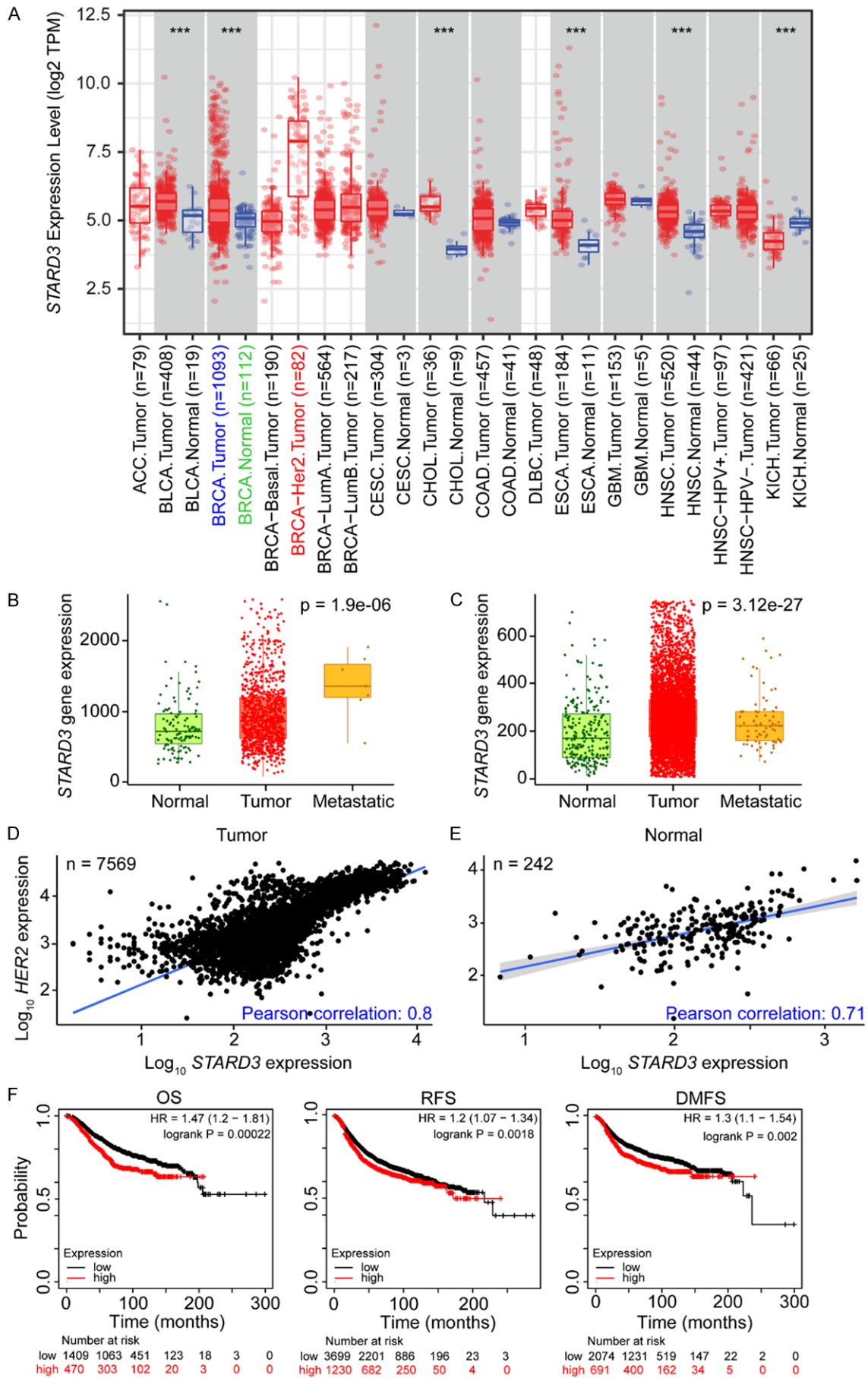
STARD3-mediated regulation of HER2 promotes breast cancer progression

Figure 2. Using TCGA and Kaplan-Meier Plotter database to analyze the clinical prognosis of STARD3 and HER2 expression in BC tumor tissue. (A) Timer 2.0 of the TCGA database analyzed STARD3 expression between breast cancer and some other tumors and adjacent normal tissues (Wilcoxon test *P < 0.05, **P < 0.01, ***P < 0.001). (B and C) TNMplot analysis of STARD3 expression between normal, tumor, and metastatic gene array data, (B) RNA-seq from TCGA, and (C) microarray from GEO. (D and E) Pearson correlation coefficient and regression analysis of the correlation between STARD3 and HER2 expression in (D) tumor and (E) normal tissues (*P < 0.001). (F) Kaplan-Meier Plotter (KM Plotter Database) analysis of STARD3 mRNA expression correlations with Overall Survival (OS), Recurrence-Free Survival (RFS), and Distant Metastasis-Free Survival (DFMS) in a breast cancer panel.
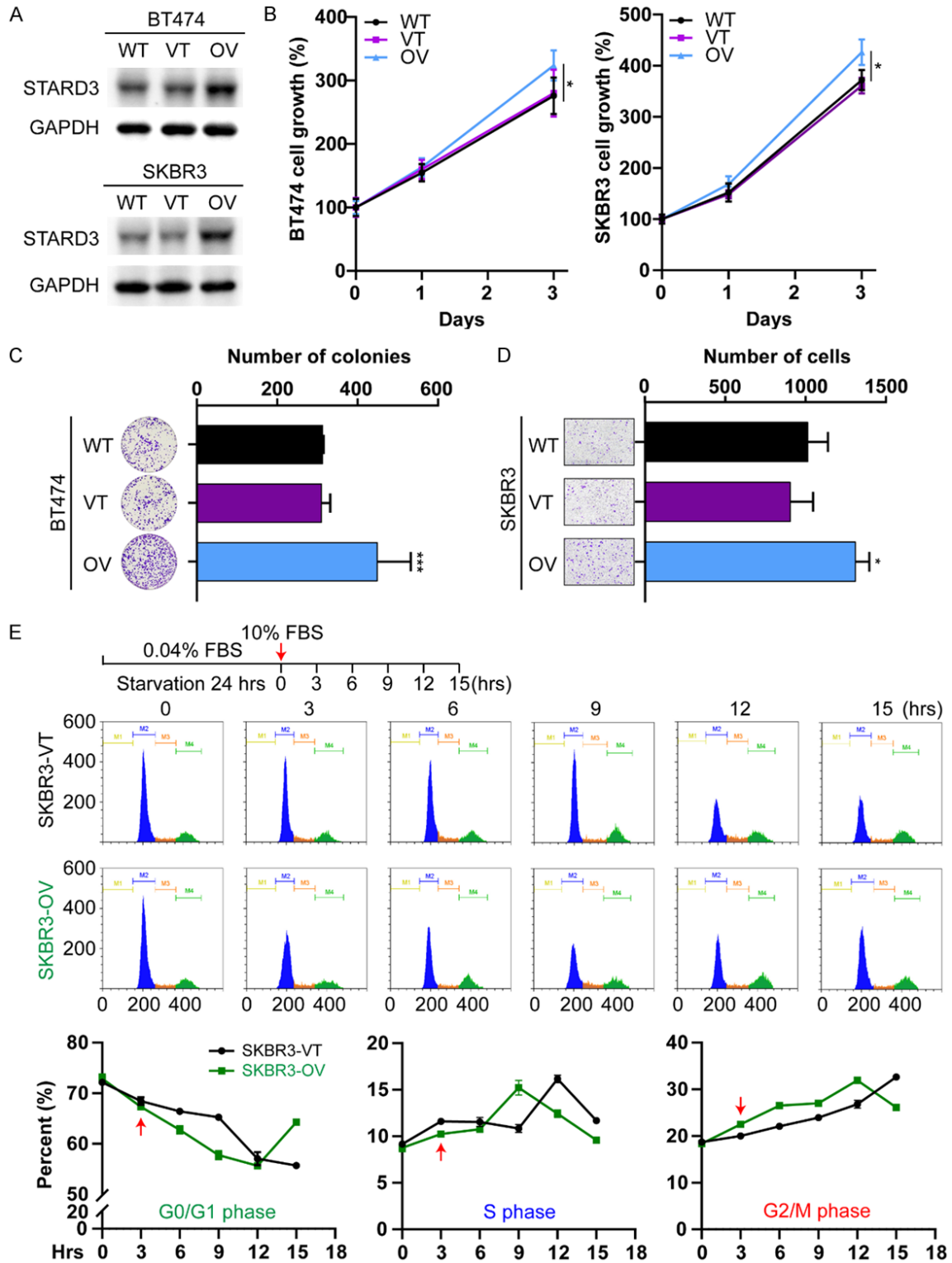
Figure 3. STARD3 overexpression promotes the malignant characterization of HER2+ cancer cells. A. Stable BT474 and SKBR3 cell lines overexpressing STARD3 protein were established. Vector control and the wild-type were controls (OV, VT, WT). B. Trypan blue assay for detection of cell proliferation in STARD3 overexpressing BT474 and SKBR3. Count the number of cells on days 1 and 3. C. Colony formation assay for detection of STARD3 overexpression in BT474-WT, VT, OV cells. Cells were fixed and stained with crystal violet after 14 days to count the colonies. D. Transwell assay for detecting STARD3 overexpression in BT474-WT, VT, OV cells. Cells were fixed and stained with crystal violet after 24 hours and counted migrated-cell numbers. E. A concept diagram of the study (Top). Cells from synchronization were released from the 10% FBS treatment, and cells were harvested every 3 h for a total of 15 h. Flow cytometry analysis determines the percentage of cell populations in different cell cycle stages (middle and low). The results were triplicated for statistics (bottom). All data are presented as mean ± SD. The *p* values were calculated using one-way ANOVA (*$P < 0.05$, ***$P < 0.001$).

We performed flow cytometry analysis in a time-dependent to elucidate further that STARD3 overexpression affects cancer cell cycle progression (**Figure 3E**, n = 3). Before evaluating cell populations at various cell growth cycle stages, we performed synchronization tests by culturing cells in 0.04% FBS for 24 hours. Afterward, stimulation with 10% FBS reactivated synchronized cells into the cell cycle [26]. We could see that SKBR3-OV cells were released from synchronization by 10% FBS treatment, cells entered G0/G1 and S phase faster than SKBR3-VT control cells, and the ratio of G0/G1 and S phase was significantly reduced from 6-9 hours. Meanwhile, the proportion of SKBR3-OV cells increased in the G2/M phase at 6-9 h compared with SKBR3-VT cells. Consistent with these results, western blot analysis confirmed increasing the cell cycle regulatory protein cyclin D1. In contrast, the protein p27 [41], which inhibits cancer cell growth, was downregulated (**Figure 4F**). These findings suggest that STARD3 overexpression promotes cell growth proliferation and migration through cell cycle regulation an oncogenic role of STARD3 in HER2+ cancer cells.

Knockdown of STARD3 attenuates HER2 cell proliferation, cell migration, and colony formation

To further evaluate whether STARD3 contributes to the malignant phenotype of HER2+ cancer cells, we performed knockdown experiments using small interfering RNA (siRNA) targeting STARD3. First, we established the stable STARD3 knockdown (STARD3-si) and the scramble (Sc) cells as control. Western blot was used to confirm protein expression (**Figure 4A**). STARD3 knockdown dramatically reduced cell proliferation in HCC1954 and BT474 cells compared to scramble and wild-type cells (**Figure 4B**). Also, STARD3-si cells exhibited a significant inhibition of cells forming colonies com-

pared to control cells (**Figure 4C**). HCC1954 cells were then subjected to a wound-healing migration assay. **Figure 4D** showed that the cell migration ability of STARD3-si cells was substantially lower than that of scramble and wild-type cells. In addition to analyzing the malignant behavior changes of cancer cells, we further explored the expression of proteins related to cell growth and survival. Western blot analysis in **Figure 4E** demonstrated that the knockdown of STARD3 in HER2 cells significantly downregulated cyclin D1 and HER2 downstream signals such as phosphorylated AKT. Previous studies have shown that SRC is a protein kinase-mediated signaling pathway that can interact with various membrane proteins, including HER2 [42]. Our study found that STARD3 knockdown cells had significantly reduced phosphorylated SRC (pSRC) levels. Moreover, we observed a concomitant increase in the expression of the cell cycle inhibitor protein p27 (**Figure 4E**). To further validate these findings, we transfected BT474 and SKBR3 breast cancer cells with STARD3 overexpression plasmid. We assessed the effects of STARD3 on the expression of these proteins involved in cell growth and survival (**Figure 4F**). **Figure 4E** and **4F** demonstrated that STARD3 expression activated the signaling proteins associated with cell proliferation and survival, indicating that STARD3 protein is critical for the malignant behavior of HER2+ breast cancer cells and plays a key role.

STARD3 regulates and stabilizes HER2 expression at the protein level through interaction with HSP90 and lysosomal degradation

As mentioned above, the expression of STARD3 was positively correlated with the HER2 protein level in BC cells. However, the biological mechanism by which STARD3 interacts with HER2 remains unclear, prompting us to investigate how STARD3 affects HER2 protein. In fact,
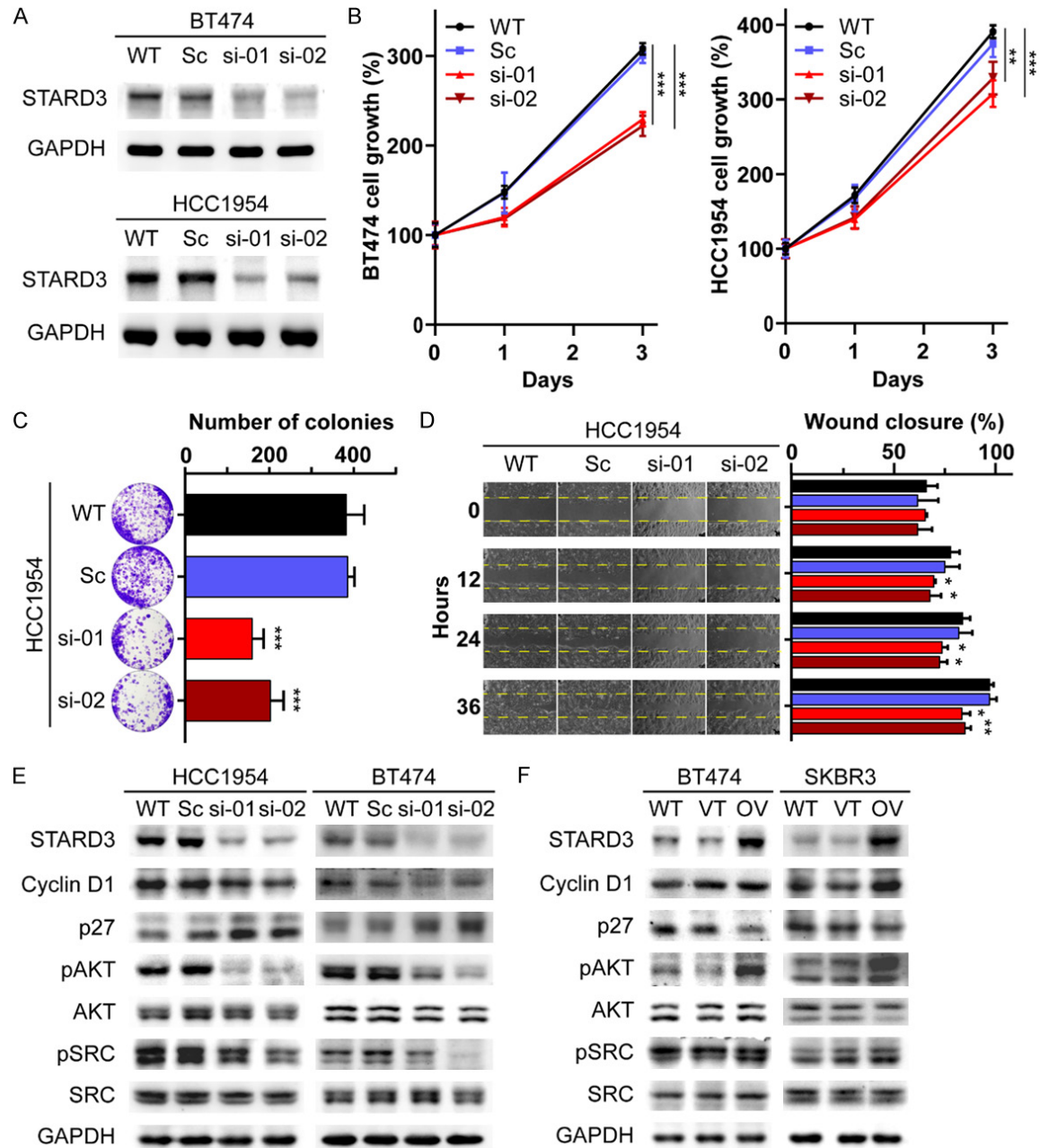
Figure 4. STARD3 inhibition attenuates malignant features of HER2+ breast cancer cells. (A) Stable BT474 and HCC1954 cell lines inhibiting STARD3 protein were established. Scrambled sequence and wild-type are controls (Si, Sc, WT). (B) Trypan blue assay for detection of cell proliferation in STARD3-silenced BT474 and HCC1954. Count the number of cells on Day 1 and Day 3. (C) Examination of how STARD3 inhibition in HCC1954-si, WT, and Sc cells affects colony formation. Cells were fixed and stained with crystal violet after 14 days to count the colonies. (D) Wound healing assay in HCC1954-si, WT, and Sc cells using Culture-Insert 2 Well. Calculate the wound closure rate at 12, 24, and 36 h. (E and F) The expression of cell cycle regulatory proteins and cell survival-related signaling proteins were detected by Western blot in (E) STARD3 knockdown HCC1954 and BT474 cells and (F) STARD3 overexpression BT474 and SKBR3 cells. GAPDH was used as an internal control protein. All data are shown as mean ± SD. The p values were calculated using one-way ANOVA ($*P < 0.05$, $**P < 0.01$, $***P < 0.001$).

western blot analysis showed that knockdown of STARD3 significantly reduced HER2 expression compared with wild-type and scrambled-type (**Figure 5A**). Meanwhile, HER2 protein levels were significantly increased in STARD3-overexpressing cells (**Figure 5B**), suggesting
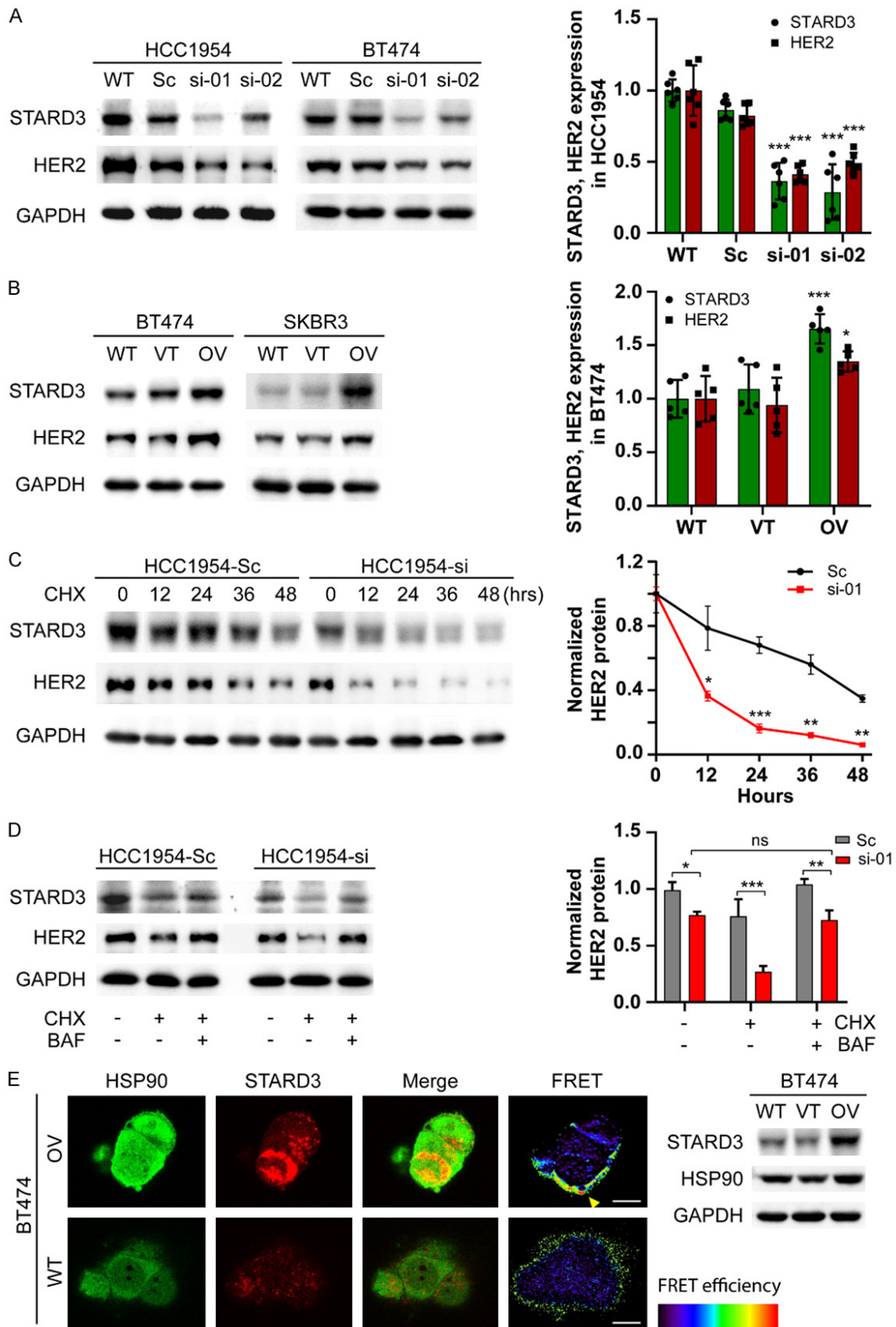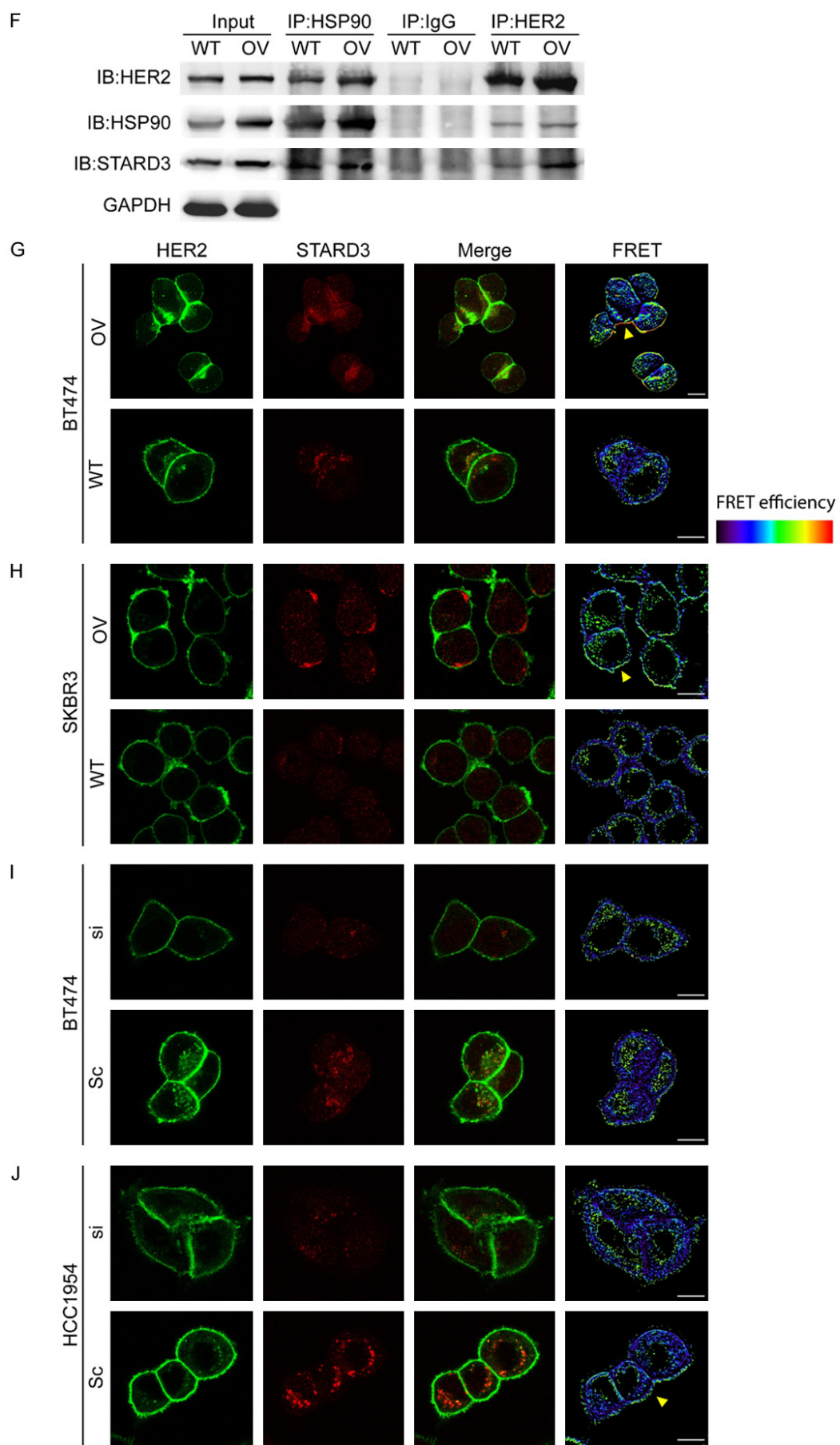
Figure 5. STARD3 expression plays an essential role in maintaining HER2 protein stability. (A, B) HER2 expression was detected in (A) STARD3 knockdown HCC1954 cells and (B) STARD3 overexpression BT474 cells by western blot. (C) HER2 protein levels in HCC1954-sc and HCC1954-si cells treated with cycloheximide (CHX) using western blot. HER2 expression was normalized with GAPDH, and its expression at time point 0 h served as a basal level control, as shown in the right panel. (D) HCC1954-Sc and HCC1954-si cells were pretreated with 20 nM BAF for 4 h before being treated for 24 hours with or without 20 μM CHX. Quantification of HER2 protein levels was normalized using GAPDH, as described in (C), shown on the right. (E) FRET activity assay of STARD3/HSP90 protein-protein interaction in BT474-OV cells. Western blot analysis of STARD3 and HSP90 is shown in the right panel. (F) Co-immunoprecipitation (CoIP) analysis was performed to test the interaction between HER2 and HSP90 in BT474-OV cells. Whole-cell lysates were used as input controls. Immunoprecipitation was performed using anti-HSP90 antibody (IP:HSP90) and anti-HER2 antibody (IP:HER2), respectively. (G-J) FRET activity assay detecting STARD3/HER2 interaction in (G, H) STARD3 overexpression cells and (I, J) STARD3 knockdown cells. Cells transfected with scrambled sequences served as controls. Scale bar = 36.8 μm. All data are shown as mean ± SD. The p values were calculated using a two-tailed unpaired Student's t-test (*$P < 0.05$, **$P < 0.01$, ***$P < 0.001$).

that changes in STARD3 may affect HER2 stability. We performed qRT-PCR analysis to investigate whether STARD3 regulated HER2 at the transcriptional level. Neither knockdown nor overexpression of STARD3 affected HER2 mRNA levels significantly (Figure S1F), indicating that the modulation of HER2 protein levels by STARD3 was not due to changes in HER2 mRNA expression. Further studies are necessary to elucidate the molecular mechanisms through which STARD3 influences HER2 expression.

To further assess the effectiveness of STARD3 on HER2 stability, we performed a CHX chase assay using the protein synthesis inhibitor cycloheximide. STARD3-si and Sc cells were treated with 20 μM CHX at indicated time points (**Figure 5C**). As expected, HER2 and STARD3 protein levels decreased slowly in a time-dependent manner in scramble cells (Figure S1E). In contrast, the degradation of HER2 was more pronounced in HCC1954-si cells after CHX treatment. These results imply increased stability of HER2 in the presence of STARD3.

We next explored whether lysosomes are involved in HER2 degradation mediated by STARD3 knockdown. Pretreated HCC1954-si cells 20 nM of BAF (lysosomal inhibitor bafilomycin A1) for 4 hours and then co-treated with 20 μM CHX and BAF for 24 hours. Interestingly, we found that CHX treatment rapidly decreased HER2 protein in STARD3 knockdown (HCC1954-si) cells compared to scrambled control (HCC1954-sc) cells. Meanwhile, the lysosomal inhibitor BAF could restore the reduced HER2 levels (**Figure 5D**), suggesting that STARD3 protects HER2 from lysosomal degradation.

A chaperone system consisting of heat shock protein 90 (HSP90) has been shown to protect client proteins, including HER2, from ubiquitin-mediated endocytosis [43]. Interestingly, STARD3 overexpression in BT474 breast cancer cells showed higher HSP90 and STARD3 fluorescence signals than wild-type cells under the same conditions (**Figure 5E**). Therefore, we further investigated whether there was an interaction between these two proteins. A photobleaching FRET assay was performed to test whether STARD3 interacts with HSP90 proteins. The results showed that a significant FRET activity signal was detected in STARD3 overexpressing cells (**Figure 5E**, yellow arrow), implying that STARD3 overexpression could enhance the interaction with HSP90 and promote HER2 protective ability.

To demonstrate the effect of STARD3 on HER2/Hsp90 interaction, we conducted CoIP analysis on BT474 wild-type and STARD3 overexpression cells. Immunoprecipitation with anti-HER2 antibody (IP:HER2) revealed an increased presence of HSP90 in the immunoprecipitated complex, and immunoprecipitation HSP90 showed an increase in HER2 (**Figure 5F**), further confirming the enhanced HER2/HSP90 interaction mediated by STARD3. These findings suggest that STARD3 plays a crucial role in facilitating the interaction between HER2 and HSP90, potentially influencing the stability or function of the HER2 protein complex.

Furthermore, overexpression of STARD3 significantly increased the direct interaction of STARD3 and HER2 in BT474-OV and SKBR3-OV cells (**Figure 5G**, **5H**). In contrast, STARD3 knockdown (Si) showed a lower FRET activity signal than that of scrambled sequence (Sc) control cells (**Figure 5I**, **5J**). Our results suggest

that overexpression of STARD3 in HER2+ cancer cell lines may stabilize HER2 protein expression through direct interactions with HER2 and HSP90. Importantly, loss of STARD3 protein expression resulted in HER2 degradation, as described above (**Figure 5A-C**). Such results suggest that targeting STARD3 protein expression in breast cancer cells could serve as a new cancer treatment strategy.

Curcumin attenuates the proliferation of HER2 cells by inhibiting the expression of STARD3 and HER2

Based on our findings on the crucial role of STARD3 in cancer development, STARD3 has the potential to be a promising target for cancer therapy. However, there are only two reports of virtual screening studies on its inhibitors using STARD3 as a target molecule and designing drugs [21, 22]. Combining natural compounds with tumor drugs is a relatively safe and effective strategy. This study used various potential natural compounds to target STARD3 expression in HER2+ cancer cells. Curcumin effectively decreased STARD3 protein levels in cancer cells using western blot analysis in three HER2 cell lines (**Figure 6A**). To examine the cytotoxicity of curcumin in HER2+ cell lines, an MTT assay was performed, and MCF-10A was used as a control group for normal cells. As shown in **Figure 6B**, curcumin affects different cells differently. HCC1954 cells are more sensitive than BT474, and the inhibitory concentrations (IC_{50}) are 14.35 and 37.0, respectively. In contrast, no significant cytotoxic effect was observed on MCF-10A cells (**Figure 6C**). To evaluate the time further- and dose-dependent effects of curcumin on STARD3 protein expression, HCC1954 and BT474 cells were treated with curcumin in a dose- and time-dependent. Western blot analysis showed that curcumin inhibited STARD3 expression in both cells (**Figure 6D**). Furthermore, **Figure 6E** showed that 15 µM curcumin inhibited cell proliferation while reducing STARD3 and HER2 protein levels (**Figure 6D**). Our findings show that curcumin might be a promising natural cancer treatment through inhibiting STARD3 and HER2 expression in HER2+ cancer cells.

Knockdown of STARD3 synergizes the cytotoxic effect of curcumin in HER2 cell lines

Knockdown of STARD3 weakened the stability of HER2, and curcumin could inhibit the expression of STARD3. We expect whether clinical treatment with curcumin can achieve a synergistic anti-tumor effect by inhibiting STARD3. To assess this hypothesis, we treated STARD3-si breast cancer cells with the indicated doses of curcumin and examined its inhibitory effect on cell viability, colony formation, and migration. As shown in **Figure 7A**, the STARD3-si cell viability was dramatically reduced compared to the wild-type and scrambled sequence controls. Notably, the knockdown of STARD3 resulted in cells more sensitive to curcumin, which prompted us to examine the growth inhibitory effect by clonogenic survival assay (**Figure 7B**). No remarkable difference was seen between the untreated and 0.1 µM curcumin groups. The substantial difference began with the 1 µM curcumin group and was strongest in the 5 µM curcumin group.

In the cell migration assay, 15 µM curcumin significantly inhibited the STARD3-si cell from migrating and even induced cell death. In contrast, the scramble cells had a less inhibitory effect (**Figure 7C**). Western blot analysis confirmed that STARD3-si cells in the curcumin-treated group showed significantly suppressed HER2 levels compared with control cells (**Figure 7D**). HER2 protein in each group was normalized and shown in the right panel. We found that the downstream signaling pathway pAKT protein, cell cycle regulatory protein Cyclin D1, and pSRC were significantly reduced in STARD3-si cells treated with curcumin. Simultaneously, p27, a cyclin-dependent kinase (CDK) inhibitor, was significantly induced (**Figure 7D**). In contrast, the expression of these proteins was not apparent in the cells of the scramble group.

To assess synergy, the coefficient of drug interaction (CDI) was examined according to the formula shown, where STARD3-si is drug A, and curcumin is drug B [44]. As shown in **Table 2**, curcumin treatment in combination with STARD3 knockdown induced significant inhibitory effects on cell viability, colony formation, and cell migration. Notably, curcumin treatment of HCC1954-si cells showed a strong synergistic effect (CDI less than 0.7) even at 5 µM curcumin. Interestingly, we observed a synergistic effect in the protein levels of key markers, including HER2, cyclin D1, p27, pAKT, and pSRC. The CDI value was less than 1, indicating a synergistic interaction between curcumin treatment and STARD3 knockdown (Table S2).
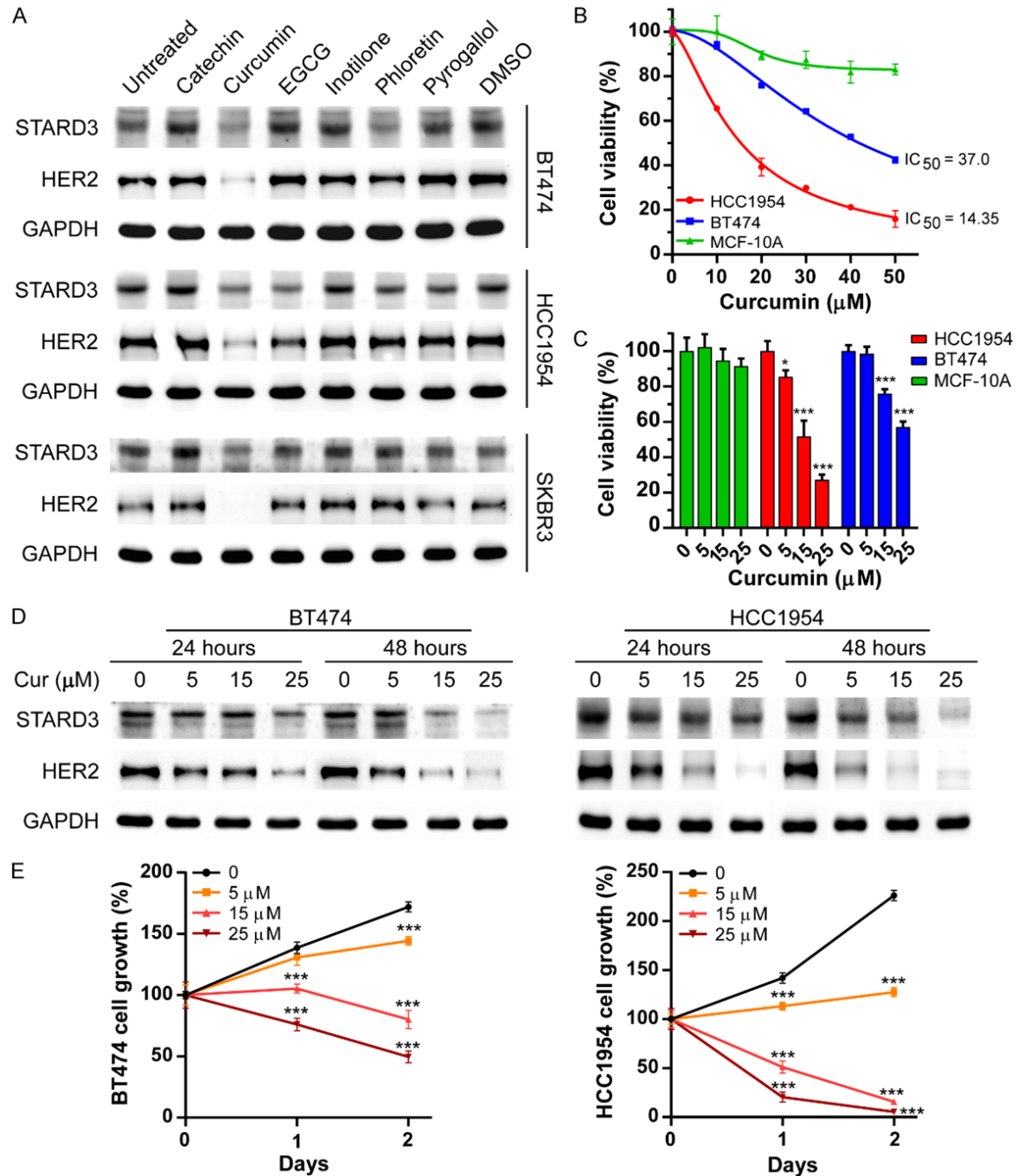
Figure 6. Curcumin treatment inhibits STARD3-mediated HER2+ cell growth. A. HER2+ cells were treated with natural compounds (25 μM) for 24 hours. STARD3 and HER2 expression was detected by western blot. DMSO was used as a vehicle. GAPDH was used as an internal control. B. Cell viability detected IC_{50} of HCC1954, BT474, and MCF-10A using an MTT assay. C. The confirmation of cell viability using the Trypan blue cell counter on HCC1954, BT474, and MCF-10A. D. Treated BT474 and HCC1954 cells in a dose- and time-dependent manner of curcumin (0-25 μM) for 24 and 48 hours. Western blot results displayed the protein levels of STARD3 and HER2. E. Cell proliferation assay of curcumin treatment on BT474 and HCC1954 cells. Cell number was counted on day 1 and day 2 of treatment using Trypan blue. The *p* values were calculated using two-way ANOVA (*P < 0.05, **P < 0.01, ***P < 0.001).

Collectively, this study demonstrates that STARD3 knockdown cells attenuate to HER2 cell lines and that curcumin exposure produces a synergistic therapeutic effect. Our findings imply that curcumin at appropriate doses has the potential to serve as a novel therapeutic
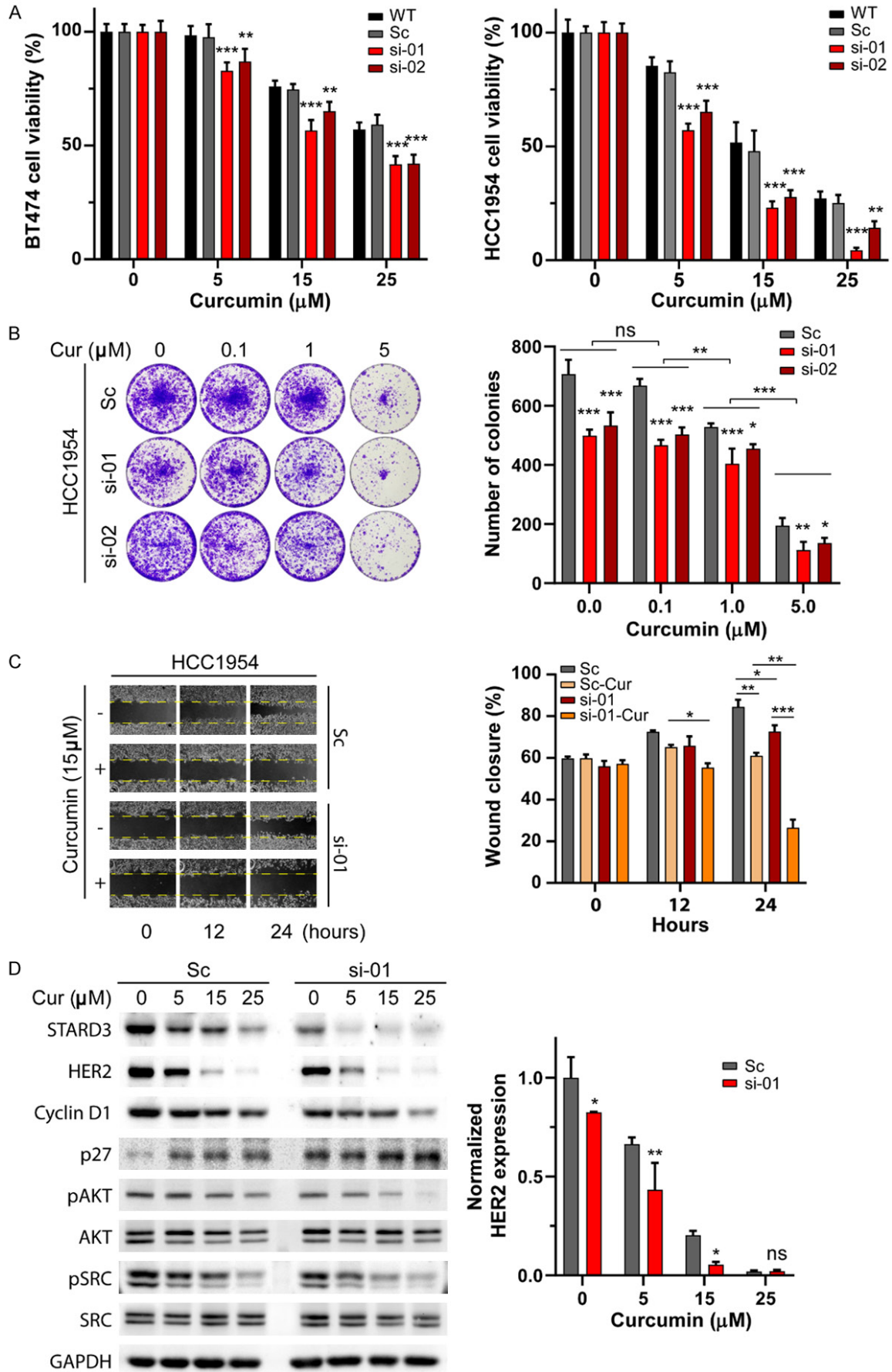
Figure 7. Synergistic effect of curcumin combination treatment on STARD3 knockdown cells. A. Cell viability was calculated using trypan blue after curcumin treatment of STARD3 knockdown BT474 and HCC1954 cells for 24 hours. B. After 14 days of treating HCC1954-si and scrambled sequence cells with curcumin, fixed cells with 4% paraformaldehyde and 0.5% crystal violet were used to stain cells as indicated by the colony formation assay. The right panel represents the number of colonies counted. C. A wound healing assay of curcumin-treated HCC195-si stable cells. HCC1954-Sc was used as a control. The right panel represents the wound closure rate of HCC1954-si and HCC1954-Sc cells after 24 hours of treatment. D. Treated HCC1954-si and Sc cells with curcumin for 24 hours. The expression of STARD3, HER2, and their related proteins were examined using a western blot. GAPDH was used as an internal control. HER2 protein expression in curcumin-treated cells was normalized with GAPDH and then normalized with untreated cells shown in the right panel. The *p* values were calculated using two-way ANOVA (*$P < 0.05$, **$P < 0.01$, ***$P < 0.001$).

Table 2. The coefficient of drug interaction (CDI) between curcumin and STARD3 knockdown cells

	Cell viability assay							
	si-01	Cur	Combination	CDI	si-02	Cur	Combination	CDI
BT474								
5 µM	0.87	0.98	0.72	0.84	0.84	0.98	0.73	0.88
15 µM	0.87	0.86	0.49	0.74	0.84	0.86	0.55	0.86
25 µM	0.87	0.57	0.36	0.73	0.84	0.57	0.35	0.74
HCC1954								
5 µM	0.73	0.85	0.41	0.67	0.84	0.85	0.52	0.76
15 µM	0.73	0.52	0.17	0.44	0.84	0.52	0.22	0.54
25 µM	0.73	0.27	0.00	0.16	0.84	0.27	0.11	0.52
Clonogenic assay								
0.1 µM	0.71	0.95	0.66	0.99	0.75	0.95	0.71	1.00
1 µM	0.71	0.75	0.57	1.08	0.75	0.75	0.64	1.14
5 µM	0.71	0.28	0.16	0.82	0.75	0.28	0.19	0.93
Cell migration								
0 h	0.94	1.00	0.96	1.02				
12 h	0.91	0.90	0.76	0.94				
24 h	0.86	0.72	0.31	0.50				

strategy for HER2+ breast cancer patients with high STARD3 expression.

Discussion

Recent studies demonstrated the potential role of co-amplified genes with HER2, such as TOP2A, GRB7, and STARD3, which may contribute to HER2 therapy resistance through various mechanisms [8]. STARD3 was reported to be co-amplified with HER2, and high levels of STARD3 are correlated to metastasis, poor prognosis, and a diminished response to trastuzumab [13, 40, 45]. However, the mechanism by which STARD3 associates with HER2 and drives cancer cells remains unclear. Peretti et al. [14] hypothesized that when STARD3 is over-expressed, ER wraps around endosomal membranes and creates membrane contact sites, causing endosomes to lose their kinetic and transient characteristics. Excess ER-late endo-

some (LE) topology might lead to locking LE and prevents their maturation into lysosomes. This condition inhibits lysosomal degradation of cell surface receptors, including HER2 and other surface receptors. Therefore, since the termination signal has been inhibited, the receptor would recover, resulting in uncontrolled cancer cells. However, this hypothesis has not been elucidated. Our study reveals that STARD3 potentiates the regulation of HER2 via direct STARD3/HER2, STARD3/HSP90 interaction and promotes SRC, thereby driving HER2 cancer cell growth and metastasis.

Genetically, STARD3 is located on the long arm of chromosome 17, close to HER2, and shares the same transcription factor SP1. As such, it is frequently co-amplified with HER2 and is highly expressed in breast cancer tumors [8]. In a cohort of 153 patients, we analyzed paired breast tumors and adjacent normal tissue, giv-

ing results consistent with high expression of STARD3 mRNA in tumors, especially HER2+ BC tumors (**Figure 1A-C**). In addition, we found higher STARD3 protein levels in HER2+ tumor tissues and HER2 cell lines compared with TNBC and luminal subtypes. We generated STARD3-overexpressing cells (BT474 and SKBR3) and STARD3-knockdown stable cell lines (HCC1954 and BT474) as research platforms to study STARD3 oncogenicity. As expected, STARD3 overexpressing cells promoted HER2 cell proliferation, migration, and colony formation. Concurrently, the knockdown of STARD3 attenuated cell growth and inhibited cell migration and colony formation. Thus, STARD3 may contribute to the progression of HER2+ breast cancer.

Our study presents the first investigation of the molecular mechanism underlying the interaction between HER2 and STARD3, which had not been previously explored in previous studies [19, 22]. STARD3 knockdown reduced HER2 levels, whereas overexpression of STARD3 elevated HER2 expression (**Figure 5A**, **5B**). HER2 was rapidly degraded upon STARD3 loss and restored by lysosomal inhibition, suggesting that STARD3 can protect HER2 from lysosomal degradation (**Figure 5C**, **5D**). Heat shock protein 90 is an essential chaperone protein with higher expression in cancer cells. Its critical functions are correct folding, stabilization, activation, and protection of several client proteins, including SRC, ATK, and HER2, which have crucial features in cancer cell proliferation and survival signaling pathways [46]. Our results showed that overexpression of STARD3 increased HSP90 levels and enhanced direct STARD3/HSP90 interaction, thereby stabilizing HER2 (**Figure 5E**).

STARD3 protein is mainly localized in the endosomal membrane, and its function is to transport cholesterol from the plasma membrane or endoplasmic reticulum to the LE [15]. Recent studies have shown that STARD3 is frequently observed in the plasma membrane of cells with high STARD3 protein levels [19]. This observation explains our findings of increased FRET activity between STARD3 and HER2 in STARD3-overexpressing cells (**Figure 5F**, **5G**). Thus, STARD3 may regulate and stabilize HER2 expression at the protein level through interaction with HSP90 and lysosomal degradation.

Therefore, STARD3 may serve as a promising molecular target in HER2+ BC, and our findings may serve as the basis for future drug design for targeted therapy.

Although HER2-targeted therapies have improved survival in patients with HER2+ BC, drug resistance still occurs frequently. Therefore, it is essential to understand the mechanism and develop new therapeutic strategies [3]. SRC, a tyrosine kinase protein associated with HER2, was reported to be promoted trastuzumab-resistant [42, 47]. Our results indicated that pSRC expression was decreased in STARD3 knockdown cells and that curcumin treatment synergistically suppressed pSRC expression. In contrast, overexpression of STARD3 increased activated pSRC (**Figures 4E**, **7D**), suggesting that STARD3 expression may be involved in HER2-targeted therapy resistance. Although STARD3 is essential to cancer development and is recognized as a novel biomarker [5, 20], study on STARD3 inhibitors as a cancer therapy is still limited [22]. Our research showed that curcumin inhibits the growth of cancer cells by inhibiting the expression of STARD3 and HER2. Furthermore, curcumin treatment combined with the knockdown of STARD3 showed significant synergy in inhibiting cell proliferation, migration, and colony formation. Both our results and previous reports show that curcumin, a natural compound with anti-cancer potential, has clinical potential to enhance anti-tumor chemotherapy with minimal side effects [23].

Altogether, our study suggests an underlying molecular mechanism by which STARD3 regulates HER2. The overexpression of STARD3 can increase the level of HER2 and increase the phosphorylation of SRC through the interaction with HSP90, thereby promoting the HER2 downstream signaling pathway-related protein pAKT to promote cell proliferation, survival, and migration. Furthermore, overexpression of STARD3 represses p27 and elevates cyclin D1, resulting in accelerated cell cycle progression. In contrast, the knockdown of STARD3 showed reversible results, with the combination with curcumin treatment significantly enhancing synergistic inhibition of HER2 cancer cells (**Figure 8**). Our findings also assist clinicians in further evaluating the correlation between STARD3
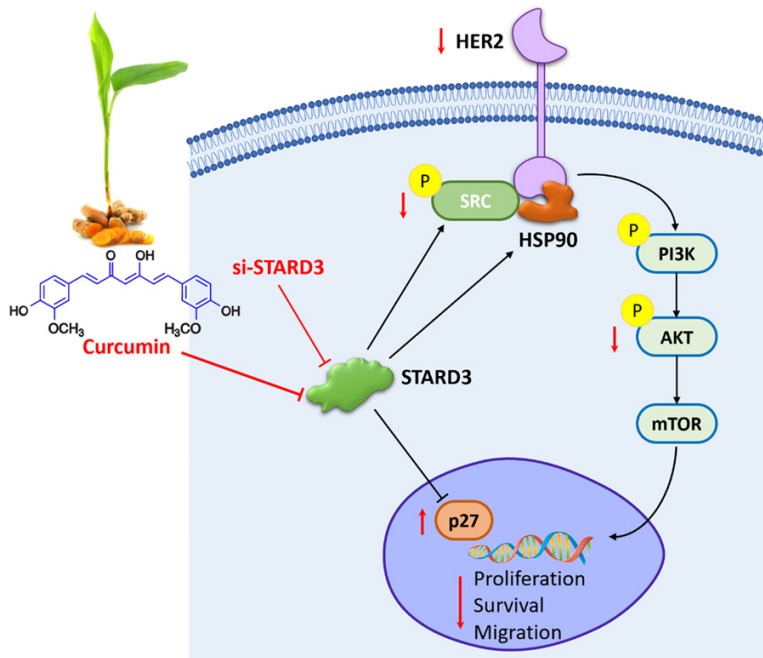
Figure 8. Graphic abstract. The red annotations indicated that STARD3 knockdown or/and curcumin treatment affected the related proteins.

overexpression and the prognosis of HER2 therapy-resistant breast cancer patients.

Conclusion

In conclusion, our work describes the molecular mechanism for the first time by which STARD3 regulates HER2 expression, drives cancer cell cycle progression, and contributes to clinical outcomes. We also found that STARD3 could be co-expressed with HER2 protein and associated with poor outcomes, suggesting that STARD3 is a crucial biomarker of clinical prognosis. Therefore, targeting STARD3 is a promising therapeutic strategy. Since there are currently no STARD3-targeting drugs, our research suggests that curcumin could be a potent natural STARD3 inhibitor. Our findings suggest an innovative therapeutic suggestion for HER2 therapy-resistant patients by targeting STARD3.

Acknowledgements

Disclosure of conflict of interest

None.

Abbreviations

AKT, Protein kinase B; BAF, Bafilomycin A1; BC, Breast cancer; CDI, Coefficient of Drug Interaction; CDK, Cyclin-Dependent Kinase; CHX, Cycloheximide; DMFS, Distant Metastasis-Free Survival; EGCG, Epigallocatechin gallate; ER, Endoplasmic reticulum; FRET, Fluorescence Resonance Energy Transfer; GAPDH, Glyceraldehyde 3-phosphate dehydrogenase; GEO, Gene Expression Omnibus; GLOBOCAN, Global Cancer Incidence, Mortality, and Prevalence; GRB7, Growth factor Receptor-Bound protein 7; HER2, Human Epidermal growth factor Receptor 2; HER2+, HER2-positive; HSP90, Heat Shock Protein 90; LE, Late Endosomes; MLN64, Metastatic Lymph Node clone 64; MTT, 3-(4,5-dimethylthiazol-2-yl)-2,5 diphenyl tetrazolium bromide; NF-κB, Nuclear Factor Kappa B; OS, Overall Survival; qPCR, Quantitative Polymerase Chain Reaction; PI3K, Phosphoinositide 3-kinases; RARA, Retinoic Acid Receptor Alpha; RFS, Recurrence-Free Survival; RT-PCR, Reverse Transcription PCR; SRC, Non-receptor tyrosine kinase; STARD3, StAR-related lipid transfer domain-containing protein 3; START, Steroidogenic Acute Regulatory Protein-related Lipid Transfer; TCGA, The Cancer Genome Atlas; TNBC, Triple-Negative Breast Cancer; TOP2A, Topoisomerase 2-alpha.

Address correspondence to: Li-Ching Chen, Department of Biological Science and Technology, College of Life Science, China Medical University, Taichung 406040, Taiwan. E-mail: lcchen@mail.cmu.edu.tw; Yuan-Soon Ho, Institute of Biochemistry and

Molecular Biology, College of Life Science, China Medical University, Taichung 406040, Taiwan. E-mail: hoyuansn@mail.cmu.edu.tw

References

[1] Giaquinto AN, Sung H, Miller KD, Kramer JL, Newman LA, Minihan A, Jemal A and Siegel RL. Breast cancer statistics, 2022. CA Cancer J Clin 2022; 72: 524-541.

[2] Schlam I, Tarantino P and Tolaney SM. Overcoming resistance to HER2-directed therapies in breast cancer. Cancers (Basel) 2022; 14: 3996.

[3] Wu X, Yang H, Yu X and Qin JJ. Drug-resistant HER2-positive breast cancer: molecular mechanisms and overcoming strategies. Front Pharmacol 2022; 13: 1012552.

[4] Duro-Sánchez S, Alonso MR and Arribas J. Immunotherapies against HER2-positive breast cancer. Cancers (Basel) 2023; 15: 1069.

[5] Vassilev B, Sihto H, Li S, Holtta-Vuori M, Ilola J, Lundin J, Isola J, Kellokumpu-Lehtinen PL, Joensuu H and Ikonen E. Elevated levels of StAR-related lipid transfer protein 3 alter cholesterol balance and adhesiveness of breast cancer cells: potential mechanisms contributing to progression of HER2-positive breast cancers. Am J Pathol 2015; 185: 987-1000.

[6] Sahlberg KK, Hongisto V, Edgren H, Mäkelä R, Hellström K, Due EU, Moen Vollan HK, Sahlberg N, Wolf M, Børresen-Dale AL, Perälä M and Kallioniemi O. The HER2 amplicon includes several genes required for the growth and survival of HER2 positive breast cancer cells. Mol Oncol 2013; 7: 392-401.

[7] Furrer D, Dragic D, Chang SL, Fournier F, Droit A, Jacob S and Diorio C. Association between genome-wide epigenetic and genetic alterations in breast cancer tissue and response to HER2-targeted therapies in HER2-positive breast cancer patients: new findings and a systematic review. Cancer Drug Resist 2022; 5: 995-1015.

[8] Glynn RW, Miller N and Kerin MJ. 17q12-21 - the pursuit of targeted therapy in breast cancer. Cancer Treat Rev 2010; 36: 224-229.

[9] Benusiglio PR, Pharoah PD, Smith PL, Lesueur F, Conroy D, Luben RN, Dew G, Jordan C, Dunning A, Easton DF and Ponder BA. HapMap-based study of the 17q21 ERBB2 amplicon in susceptibility to breast cancer. Br J Cancer 2006; 95: 1689-1695.

[10] Qiu Y, Zhang ZY, Du WD, Ye L, Xu S, Zuo XB, Zhou FS, Chen G, Ma XL, Schneider ME, Xia HZ, Zhou Y, Wu JF, Yuan-Hong X and Zhang XJ. Association analysis of ERBB2 amplicon genetic polymorphisms and STARD3 expression with risk of gastric cancer in the Chinese population. Gene 2014; 535: 225-232.

[11] Fararjeh AFS, Al Khader A, Kaddumi E, Obeidat M and Al-Fawares O. Differential expression and prognostic significance of STARD3 gene in breast carcinoma. Int J Mol Cell Med 2021; 10: 34-41.

[12] Muzny DM, Bainbridge MN, Chang K, Dinh HH, Drummond JA, Fowler G, Kovar CL, Lewis LR, Morgan MB, Newsham IF, Reid JG, Santibanez J, Shinbrot E, Trevino LR, Wu YQ, Wang M, Gunaratne P, Donehower LA, Creighton CJ, Wheeler DA, Gibbs RA, Lawrence MS, Voet D, Jing R, Cibulskis K, Sivachenko A, Stojanov P, McKenna A, Lander ES, Gabriel S, Getz G, Ding L, Fulton RS, Koboldt DC, Wylie T, Walker J, Dooling DJ, Fulton L, Delehaunty KD, Fronick CC, Demeter R, Mardis ER, Wilson RK, Chu A, Chun HJE, Mungall AJ, Pleasance E, Gordon Robertson A, Stoll D, Balasundaram M, Birol I, Butterfield YSN, Chuah E, Coope RJN, Dhalla N, Guin R, Hirst C, Hirst M, Holt RA, Lee D, Li HI, Mayo M, Moore RA, Schein JE, Slobodan JR, Tam A, Thiessen N, Varhol R, Zeng T, Zhao Y, Jones SJM, Marra MA, Bass AJ, Ramos AH, Saksena G, Cherniack AD, Schumacher SE, Tabak B, Carter SL, Pho NH, Nguyen H, Onofrio RC, Crenshaw A, Ardlie K, Beroukhim R, Winckler W, Getz G, Meyerson M, Protopopov A, Zhang J, Hadjipanayis A, Lee E, Xi R, Yang L, Ren X, Zhang H, Sathiamoorthy N, Shukla S, Chen PC, Haseley P, Xiao Y, Lee S, Seidman J, Chin L, Park PJ, Kucherlapati R, Todd Auman J, Hoadley KA, Du Y, Wilkerson MD, Shi Y, Liquori C, Meng S, Li L, Turman YJ, Topal MD, Tan D, Waring S, Buda E, Walsh J, Jones CD, Mieczkowski PA, Singh D, Wu J, Gulabani A, Dolina P, Bodenheimer T, Hoyle AP, Simons JV, Soloway M, Mose LE, Jefferys SR, Balu S, O'Connor BD, Prins JF, Chiang DY, Neil Hayes D, Perou CM, Hinoue T, Weisenberger DJ, Maglinte DT, Pan F, Berman BP, Van Den Berg DJ, Shen H, Triche T Jr, Baylin SB, Laird PW, Getz G, Noble M, Voet D, Saksena G, Gehlenborg N, DiCara D, Zhang J, Zhang H, Wu CJ, Yingchun Liu S, Shukla S, Lawrence MS, Zhou L, Sivachenko A, Lin P, Stojanov P, Jing R, Park RW, Nazaire MD, Robinson J, Thorvaldsdottir H, Mesirov J, Park PJ, Chin L, Thorsson V, Reynolds SM, Bernard B, Kreisberg R, Lin J, Iype L, Bressler R, Erkkilä T, Gundapuneni M, Liu Y, Norberg A, Robinson T, Yang D, Zhang W, Shmulevich I, de Ronde JJ, Schultz N, Cerami E, Ciriello G, Goldberg AP, Gross B, Jacobsen A, Gao J, Kaczkowski B, Sinha R, Arman Aksoy B, Antipin Y, Reva B, Shen R, Taylor BS, Chan TA, Ladanyi M, Sander C, Akbani R, Zhang N, Broom BM, Casasent T, Unruh A, Wakefield C, Hamilton SR, Craig Cason R, Baggerly KA, Weinstein JN, Haussler D, Benz CC, Stuart JM, Benz SC, Zachary Sanborn J, Vaske CJ, Zhu J, Szeto C, Scott GK, Yau C, Ng S, Goldstein T, Ellrott K, Collisson E, Cozen AE,

Zerbino D, Wilks C, Craft B, Spellman P, Penny R, Shelton T, Hatfield M, Morris S, Yena P, Shelton C, Sherman M, Paulauskis J, Gastier-Foster JM, Bowen J, Ramirez NC, Black A, Pyatt R, Wise L, White P, Bertagnolli M, Brown J, Chan TA, Chu GC, Czerwinski C, Denstman F, Dhir R, Dörner A, Fuchs CS, Guillem JG, Iacocca M, Juhl H, Kaufman A, Kohl Iii B, Van Le X, Mariano MC, Medina EN, Meyers M, Nash GM, Paty PB, Petrelli N, Rabeno B, Richards WG, Solit D, Swanson P, Temple L, Tepper JE, Thorp R, Vakiani E, Weiser MR, Willis JE, Witkin G, Zeng Z and Zinner MJ; The Cancer Genome Atlas N, Genome Sequencing Center Baylor College of M, Genome Sequencing Center Broad I, Genome Sequencing Center Washington University in St L, Genome Characterization Center BCCA, Genome-Characterization Center Broad I, Genome-Characterization Center B, Women's H, Harvard Medical S, Genome-Characterization Center University of North Carolina CH, Genome-Characterization Centers University of Southern C, Johns Hopkins U, Genome Data Analysis Center Broad I, Genome Data Analysis Center Institute for Systems B, Genome Data Analysis Center Memorial Sloan-Kettering Cancer C, Genome Data Analysis Center University of Texas MDACC, Genome Data Analysis Centers UoCSC, the Buck I, Biospecimen Core Resource International Genomics C, Nationwide Children's Hospital Biospecimen Core R, Tissue source s and disease working g. Comprehensive molecular characterization of human colon and rectal cancer. Nature 2012; 487: 330-337.

[13] Vinatzer U, Dampier B, Streubel B, Pacher M, Seewald MJ, Stratowa C, Kaserer K and Schreiber M. Expression of HER2 and the coamplified genes GRB7 and MLN64 in human breast cancer: quantitative real-time reverse transcription-PCR as a diagnostic alternative to immunohistochemistry and fluorescence in situ hybridization. Clin Cancer Res 2005; 11: 8348-8357.

[14] Peretti D, Kim S, Tufi R and Lev S. Lipid transfer proteins and membrane contact sites in human cancer. Front Cell Dev Biol 2020; 7: 371.

[15] Wilhelm LP, Wendling C, Vedie B, Kobayashi T, Chenard MP, Tomasetto C, Drin G and Alpy F. STARD3 mediates endoplasmic reticulum-to-endosome cholesterol transport at membrane contact sites. EMBO J 2017; 36: 1412-1433.

[16] Tomasetto C, Régnier C, Moog-Lutz C, Mattei MG, Chenard MP, Lidereau R, Basset P and Rio MC. Identification of four novel human genes amplified and overexpressed in breast carcinoma and localized to the q11-q21.3 region of chromosome 17. Genomics 1995; 28: 367-376.

[17] Kao J and Pollack JR. RNA interference-based functional dissection of the 17q12 amplicon in breast cancer reveals contribution of coamplified genes. Genes Chromosomes Cancer 2006; 45: 761-769.

[18] Alpy F and Tomasetto CL. STARD3: a lipid transfer protein in breast cancer and cholesterol trafficking. In: Clark BJ, Stocco DM, editors. Cholesterol Transporters of the START Domain Protein Family in Health and Disease: START Proteins - Structure and Function. New York, NY: Springer New York; 2014. pp. 119-138.

[19] Voilquin L, Lodi M, Di Mattia T, Chenard MP, Mathelin C, Alpy F and Tomasetto C. STARD3: a swiss army knife for intracellular cholesterol transport. Contact 2019; 2: 251525641985673.

[20] Lodi M, Voilquin L, Alpy F, Moliere S, Reix N, Mathelin C, Chenard MP and Tomasetto CL. STARD3: a new biomarker in HER2-positive breast cancer. Cancers (Basel) 2023; 15: 362.

[21] Chitrala KN and Yeguvapalli S. Ligand-based virtual screening to predict inhibitors against metastatic lymph node 64. J Recept Signal Transduct Res 2014; 34: 92-96.

[22] Lapillo M, Salis B, Palazzolo S, Poli G, Granchi C, Minutolo F, Rotondo R, Caligiuri I, Canzonieri V, Tuccinardi T and Rizzolio F. First-of-its-kind STARD(3) inhibitor: in silico identification and biological evaluation as anticancer agent. ACS Med Chem Lett 2019; 10: 475-480.

[23] Alqahtani AM, Chidambaram K, Pino-Figueroa A, Chandrasekaran B, Dhanaraj P and Venkatesan K. Curcumin-celecoxib: a synergistic and rationale combination chemotherapy for breast cancer. Eur Rev Med Pharmacol Sci 2021; 25: 1916-1927.

[24] Zhang Y, Li H, Zhang J, Zhao C, Lu S, Qiao J and Han M. The combinatory effects of natural products and chemotherapy drugs and their mechanisms in breast cancer treatment. Phytochemistry Reviews 2019; 19: 1179-1197.

[25] Islam MR, Islam F, Nafady MH, Akter M, Mitra S, Das R, Urmee H, Shohag S, Akter A, Chidambaram K, Alhumaydhi FA, Emran TB and Cavalu S. Natural small molecules in breast cancer treatment: understandings from a therapeutic viewpoint. Molecules 2022; 27: 2165.

[26] Cheng TC, Sayseng JO, Tu SH, Juan TC, Fang CL, Liao YC, Chu CY, Chang HW, Yen Y, Chen LC and Ho YS. Curcumin-induced antitumor effects on triple-negative breast cancer patient-derived xenograft tumor mice through inhibiting salt-induced kinase-3 protein. J Food Drug Anal 2021; 29: 622-637.

[27] Chao W, Deng JS, Li PY, Kuo YH and Huang GJ. Inotilone from inonotus linteus suppresses lung cancer metastasis in vitro and in vivo

through ROS-mediated PI3K/AKT/MAPK signaling pathways. Sci Rep 2019; 9: 2344.

[28] Zargan S, Salehi Barough M, Zargan J, Shayesteh M, Haji Noor Mohammadi A, Mousavi M and Keshavarz Alikhani H. Evaluation of the anti-cancer effect of curcumin on MCF-7 cells in 3D culture conditions to increase the efficacy of breast cancer treatment. Journal of Applied Biotechnology Reports 2022; 9: 547-556.

[29] Song X, Zhang M, Dai E and Luo Y. Molecular targets of curcumin in breast cancer (Review). Mol Med Rep 2019; 19: 23-29.

[30] Farghadani R and Naidu R. Curcumin: modulator of key molecular signaling pathways in hormone-independent breast cancer. Cancers (Basel) 2021; 13: 3427.

[31] Hu S, Xu Y, Meng L, Huang L and Sun H. Curcumin inhibits proliferation and promotes apoptosis of breast cancer cells. Exp Ther Med 2018; 16: 1266-1272.

[32] Lin CY, Lee CH, Chuang YH, Lee JY, Chiu YY, Wu Lee YH, Jong YJ, Hwang JK, Huang SH, Chen LC, Wu CH, Tu SH, Ho YS and Yang JM. Membrane protein-regulated networks across human cancers. Nat Commun 2019; 10: 3131.

[33] Fararjeh AS, Chen LC, Ho YS, Cheng TC, Liu YR, Chang HL, Chang HW, Wu CH and Tu SH. Proteasome 26S subunit, non-ATPase 3 (PSMD3) regulates breast cancer by stabilizing HER2 from degradation. Cancers (Basel) 2019; 11: 527.

[34] Zhao Y, Gao JL, Ji JW, Gao M, Yin QS, Qiu QL, Wang C, Chen SZ, Xu J, Liang RS, Cai YZ and Wang XF. Cytotoxicity enhancement in MDA-MB-231 cells by the combination treatment of tetrahydropalmatine and berberine derived from Corydalis yanhusuo W. T. Wang. J Intercult Ethnopharmacol 2014; 3: 68-72.

[35] Li T, Fu J, Zeng Z, Cohen D, Li J, Chen Q, Li B and Liu XS. TIMER2.0 for analysis of tumor-infiltrating immune cells. Nucleic Acids Res 2020; 48: W509-W514.

[36] Bartha Á and Győrffy B. TNMplot.com: a web tool for the comparison of gene expression in normal, tumor and metastatic tissues. Int J Mol Sci 2021; 22: 2622.

[37] Lánczky A and Győrffy B. Web-based survival analysis tool tailored for medical research (KMplot): development and implementation. J Med Internet Res 2021; 23: e27633.

[38] Vasaikar SV, Straub P, Wang J and Zhang B. LinkedOmics: analyzing multi-omics data within and across 32 cancer types. Nucleic Acids Res 2018; 46: D956-D963.

[39] Győrffy B. Survival analysis across the entire transcriptome identifies biomarkers with the highest prognostic power in breast cancer. Comput Struct Biotechnol J 2021; 19: 4101-4109.

[40] Cai W, Ye L, Sun J, Mansel RE and Jiang WG. Expression of MLN64 influences cellular matrix adhesion of breast cancer cells, the role for focal adhesion kinase. Int J Mol Med 2010; 25: 573-80.

[41] Currier AW, Kolb EA, Gorlick RG, Roth ME, Gopalakrishnan V and Sampson VB. p27/Kip1 functions as a tumor suppressor and oncoprotein in osteosarcoma. Sci Rep 2019; 9: 6161.

[42] Luo J, Zou H, Guo Y, Tong T, Ye L, Zhu C, Deng L, Wang B, Pan Y and Li P. SRC kinase-mediated signaling pathways and targeted therapies in breast cancer. Breast Cancer Res 2022; 24: 99.

[43] Liu Z, Sang X, Wang M, Liu Y, Liu J, Wang X, Liu P and Cheng H. Melatonin potentiates the cytotoxic effect of neratinib in HER2(+) breast cancer through promoting endocytosis and lysosomal degradation of HER2. Oncogene 2021; 40: 6273-6283.

[44] Liu B, Huang X, Hu Y, Chen T, Peng B, Gao N, Jin Z, Jia T, Zhang N, Wang Z and Jin G. Ethacrynic acid improves the antitumor effects of irreversible epidermal growth factor receptor tyrosine kinase inhibitors in breast cancer. Oncotarget 2016; 7: 58038-58050.

[45] Nguyen MKL, Jose J, Wahba M, Bernaus-Esque M, Hoy AJ, Enrich C, Rentero C and Grewal T. Linking late endosomal cholesterol with cancer progression and anticancer drug resistance. Int J Mol Sci 2022; 23: 7206.

[46] Ye M, Huang W, Liu R, Kong Y, Liu Y, Chen X and Xu J. Synergistic activity of the HSP90 inhibitor ganetespib with lapatinib reverses acquired lapatinib resistance in HER2-positive breast cancer cells. Front Pharmacol 2021; 12: 651516.

[47] Vivekanandhan S and Knutson KL. Resistance to trastuzumab. Cancers (Basel) 2022; 14: 5115.

Table S1. Primers used in the study

Oligonucleotides
Primers specific for STARD3 in real-time PCR
F: 5'-GGATGGTGCTGTGGAAC
R: 5'-TCCCTGATGACAAGTAT
Primers specific for GUS in real-time PCR
F: 5'-AAACAGCCCGTTTACTTGAG
R: 5'-AGTGTTCCCTGCTAGAATAGATG
Primers specific for HER2 in real-time PCR
F: 5'-GGAAGTACACGATGCGGAGACT
R: 5'-ACCTTCCTCAGCTCCGTCTCTT
Primers specific for full-length STARD3
F: 5'-AAAAAGCTTATGAGCAAGCTGCCCAGGGA
R: 5'-AAAAAAA GGATCC TCACGCCCGGGCCCCCA
STARD3 siRNA fragments inserted into p.Super plasmid
siRNA-1F: 5'-GATCCCCGCAGGGTCTGACAATGAATTTCAAGAGAATTCATTGTCAGACCCTGCTTTTTA-3'
siRNA-1R: 5'-AGCTTAAAAAGCAGGGTCTGACAATGAATTCTCTTGAAATTCATTGTCAGACCCTGCGGG-3'
siRNA-2F: 5'-GATCCCCGGCTTCATCGTGCTCAAGTTTCAAGAGAACTTGAGCACGATGAAGCCTTTTTA-3'
siRNA-2R: 5'-AGCTTAAAAAGGCTTCATCGTGCTCAAGTTCTCTTGAAACTTGAGCACGATGAAGCCGGG-3'
STARD3 scramble siRNA fragments inserted into p.Super plasmid
F: 5'-GATCCCCCGTACGCGGAATACTTCGATTCAAGAGATCGAAGTATTCCGCGTACGTTTTTA-3'
R: 5'-AGCTTAAAAACGTACGCGGAATACTTCGATCTCTTGAATCGAAGTATTCCGCGTACGGGG-3'

STARD3-mediated regulation of HER2 promotes breast cancer progression
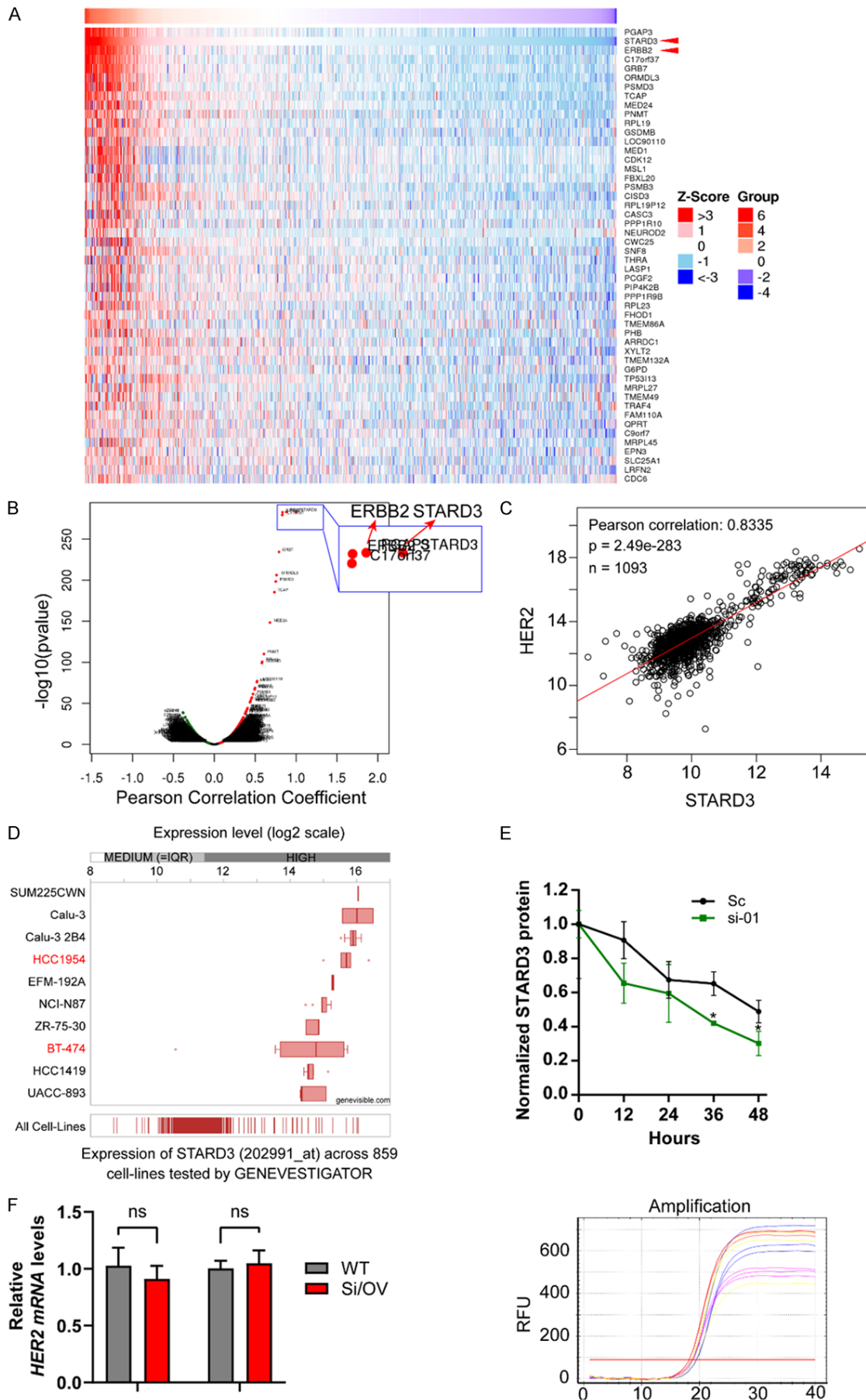
A

B

C

D

Expression of STARD3 (202991_at) across 859 cell-lines tested by GENEVESTIGATOR

E

F

2

Figure S1. Correlation between STARD3 mRNA expression and the other genes in breast cancer tumors, according to TCGA database with LinkedOmics platform analysis. A. Correlation heatmap between STARD3 mRNA expression with different genes in breast tumors. B. Volcano plot Pearson correlation of STARD3 with different genes in a positive and negative correlation. C. Pearson correlation between STARD3 and HER2 expression. D. Top 10 cell lines with the highest STARD3 expression, including HCC1954 and BT474, in Genevisible database analysis. E. STARD3 expressions were normalized with GAPDH and its expression at time point 0 in the Cycloheximide (CHX) assay **Figure 5E**. F. Impact of STARD3 knockdown/overexpression on HER2 mRNA levels in HER2 cell lines. RT-qPCR analysis of HER2 mRNA was calculated using the delta-delta Ct method ($2^{-\Delta\Delta Ct}$) to assess the relative fold gene expression. GUS was used as a housekeeping gene. The *p* values were calculated using the Student t-test (ns: not significant).

Table S2. The coefficient of drug interaction (CDI) on protein expression in **Figure 7D**

Curcumin	CDI		
	5 µM	15 µM	25 µM
STARD3	0.59	0.82	0.83
HER2	0.44	0.34	0.75
Cyclin D	0.76	0.93	0.60
p27	0.43	0.67	0.67
pAKT	1.68	0.52	0.30
pSRC	0.89	0.89	0.78